Published in final edited form as:
J Med Chem. 2013 October 24; 56(20): . doi:10.1021/jm400196q.

Synthesis and Chemical and Biological Comparison of Nitroxyl and Nitric Oxide Releasing Diazeniumdiolate-based Aspirin Derivatives

Debashree Basudhar[1], **Gaurav Bharadwaj**[1], **Robert Y. Cheng**[2], **Sarthak Jain**[3], **Sa Shi**[4,5], **Julie L. Heinecke**[2], **Ryan J. Holland**[6], **Lisa A. Ridnour**[2], **Viviane M. Caceres**[4,7], **Regina C. Spadari-Bratfisch**[7], **Nazareno Paolocci**[4,8], **Carlos A. Velázquez-Martínez**[3], **David A. Wink**[2], and **Katrina M. Miranda**[1,*]

[1]Department of Chemistry and Biochemistry, University of Arizona, Tucson, Arizona 85721

[2]Radiation Biology Branch, National Institutes of Health, Bethesda, Maryland 20892

[3]Faculty of Pharmacy and Pharmaceutical Sciences, University of Alberta, Edmonton, Canada

[4]Division of Cardiology, Department of Medicine, Johns Hopkins Medical Institutions, Baltimore, Maryland 21287

[5]Department of Pathophysiology, Harbin Medical University, Harbin, 150081, China

[6]Chemical Biology Laboratory, Frederick National Laboratory for Cancer Research, Frederick, Maryland 21702

[7]Department of Biosciences, Federal University of São Paulo (UNIFESP), Santos, SP, Brazil

[8]Department of Clinical and Experimental Medicine, University of Perugia, Perugia, Italy

Abstract

Structural modifications of non-steroidal anti-inflammatory drugs (NSAIDs) have successfully reduced the side effect of gastrointestinal ulceration without affecting anti-inflammatory activity, but may increase risk of myocardial infarction with chronic use. That nitroxyl (HNO) reduces platelet aggregation, preconditions against myocardial infarction and enhances contractility led us to synthesize a diazeniumdiolate-based HNO releasing aspirin and to compare it to an NO-releasing analogue. Here, the decomposition mechanisms are described for these compounds. In addition to protection against stomach ulceration, these prodrugs also exhibited significantly enhanced cytotoxcity compared to either aspirin or the parent diazeniumdiolate toward non-small cell lung carcinoma cells (A549) but were not appreciably toxic toward endothelial cells (HUVECs). The HNO-NSAID prodrug inhibited cylcooxgenase-2 and glyceraldehyde 3-phosphate dehydrogenase activity and triggered significant sarcomere shortening compared to control on murine ventricular myocytes. Together, these anti-inflammatory, anti-neoplasic and contractile properties suggest the potential of HNO-NSAIDs in the treatment of inflammation, cancer or heart failure.

[*]Corresponding Author: Tel: (520) 626-3655; kmiranda@email.arizona.edu.

Disclosure

Nazareno Paolocci is a founder and stockowner at Cardioxyl Pharmaceuticals Inc.

Ancillary Information

Supporting Information Available: NMR spectra showing the decomposition products of compounds **3** and **6** at pH 10; HPLC purity data for compounds **3**, **6**, **7** and **8**. This material is available free of charge via the Internet at http://pubs.acs.org.

Keywords

nitroxyl; nitric oxide; NONOate; diazeniumdiolate; IPA/NO; DEA/NO; NSAID; aspirin; COX-2; GAPDH; anti-inflammatory; anticancer; cardioprotective

Introduction

Cyclooxygenase (COX)-mediated conversion of arachidonic acid to prostaglandins affects various physiological functions, such as protection of stomach lining,[1] contraction and relaxation of smooth muscle,[2, 3] platelet aggregation,[4] renal function,[5] nerve and brain function,[6, 7] bone metabolism,[8] as well as pathological conditions, including pain, inflammation,[9] Alzheimer's disease[10-12] and cancer.[13] Use of non-steroidal anti-inflammatory drugs (NSAIDs) as COX inhibitors is extensive to reduce pain, fever and inflammation.[14] Given the diverse physiological effects of prostaglandins, NSAID treatment can lead to serious side effects including gastric ulcerogenicity and renal toxicity,[15] due in part to a lack of specificity for COX-1, which is the constitutive isoform primarily responsible for baseline formation of prostaglandins, and COX-2, which is induced during inflammation.[16] More recent studies suggest that this differentiation of the two isoforms is likely to be oversimplified, however, classic side effects of NSAIDs remain attributed to non-specific inhibition of COX.[17]

Development of later generation NSAIDs has relied on structural modification, for example to induce COX-2 selectivity or to attach a nitric oxide (NO)-donating moiety. Selective inhibitors of COX-2 (COXIBs) have successfully reduced ulcerogenicity,[18] but chronic use leads to an increased risk of heart attack and stroke.[19] COX inhibiting NO donors, CINODs or NONSAIDs[20], combine the anti-inflammatory properties of NSAIDs with the NO producing capability of nitroglycerine, which has been used for decades to treat angina and chronic heart failure.[21] These organic nitrate derivatives reduce the side effects of NSAIDs and also have efficacy as cancer therapeutics.[22] However, prolonged use can lead to nitrate tolerance as observed for nitroglycerine.[23] In addition, the dependence on metabolic pathways to produce NO from organic nitrates[24, 25] complicates measurement of NO release from CINODs. In fact, the anticancer mechanism has been suggested to involve formation of electrophilic quinone methides, which can deplete intracellular glutathione (GSH) levels, rather than production of NO.[26]

More recently, NO releasing NSAIDs have been produced by derivatization of secondary amine diazeniumdiolates (NONOates),[27, 28] which are widely used as NO donors.[29] Such NONO-NSAIDs are enzymatically cleaved to induce spontaneous release of NO from the diazeniumdiolate moiety,[27, 28] thus removing dependence on the metabolic pathways required for production of NO from organic nitrates. Another attractive attribute of secondary amine diazeniumdiolates in terms of NO donation is the ability to tune the rate of decomposition based on amine identity.[30]

Decomposition of diazeniumdiolates can also lead to nitroxyl (HNO) production.[31-33] HNO has emerged as an important pharmacological agent with beneficial effects in overcoming heart failure,[34] preconditioning against myocardial infarction,[35] decreasing tumor growth[36] and treating alcohol abuse.[37] We have recently analyzed the pH-dependent mechanisms of production of NO and HNO during decomposition of Angeli's salt ($Na_2N_2O_3$), which is the most commonly used donor of HNO, and isopropylamine diazeniumdiolate (IPA/NO).[33] For these related compounds, protonation of the terminal nitroso nitrogen, by tautomerization of the amine proton for example (Scheme 1), induces cleavage of the diazenium bond to produce HNO. In contrast, protonation of the atom attached to the diazeniumdiolate moiety

leads to separation of the NO dimer from the nucleophile. Primary amine based diazeniumdiolates can function as dual donors of NO and HNO in the pH range where both pathways are kinetically competitive. For instance, IPA/NO is an NO donor at pH ≤ 5, an HNO donor at pH ≥ 8 and a dual donor at intermediate pH.

Derivatization of amine-based diazeniumdiolates facilitates purification and increases stability in neutral and acidic conditions.[38,39] There are now numerous examples of esterified secondary amine diazeniumdiolates, and these compounds can typically be readily deprotected by esterases either within cells or upon addition of purified protein or blood serum.[30] Our recent examination of the acetoxymethyl derivative of IPA/NO (IPA/NO-AcOM) demonstrated that porcine live esterase catalyzed dissociation of free IPA/NO.[39] However, spontaneous hydrolysis of IPA/NO-AcOM unexpectedly increased HNO production over the parent diazeniumdiolate via removal of the amine proton to produce a unique intermediate (see Scheme 3 below).

Here, two new NONO-NSAIDs were prepared by derivatizing both a primary and secondary diazeniumdiolate with aspirin to produce O^2-(acetylsalicyloyloxymethyl)-1-(N-isopropylamino)-diazen-1-ium-1,2-diolate (IPA/NO-aspirin) and O^2-(acetylsalicyloyloxymethyl)-1-(N,N-diethylamino)-diazen-1-ium-1,2-diolate (DEA/NO-aspirin). Their chemical and biological properties are compared to determine the efficacy of these compounds as analgesic and anti-inflammatory agents. Additionally, the ability to induce HNO-mediated effects such as inhibition of thiol-containing proteins and enhancement of contractility was investigated.

Results and Discussion

The half-life under physiological conditions of IPA/NO (5.7 min) is comparable to that of DEA/NO (2.5 min),[29] thus facilitating comparison of these related respective HNO and NO donors. O^2-Modification of both IPA/NO and DEA/NO has previously been described,[38-40] as have the syntheses of NSAID derivatives of secondary amine diazeniumdiolates.[27, 28] Here, IPA/NO-aspirin and DEA/NO-aspirin were newly synthesized by minor modifications of published procedures (Scheme 2).[27, 41] Briefly, each amine was first exposed to a high pressure of NO to obtain the corresponding diazeniumdiolate. The desired products were produced by O^2-methylthiomethyl derivatization followed by reaction with sulfuryl chloride to produce the O^2-chloromethyl protected diazeniumdiolate, and finally by coupling with aspirin.

Decomposition mechanism

Previously, examination of the decomposition of IPA/NO-AcOM established two independent pathways for spontaneous and esterase-mediated hydrolysis.[39] Assuming these pathways are also accessible for the related aspirin derivative, spontaneous decomposition of IPA/NO-aspirin (**3**) may be initiated by deprotonation of the amine proton (**3a**), which leads to 1-4 acyl migration via a cyclic intermediate (**3b**) and expulsion of formaldehyde (Scheme 3). The resulting intermediate (**3c**) should then be susceptible to fragmentation by N-N bond cleavage to produce a reactive diazoate ion (**10**) and an acyl nitroso derivative. The acetyl group of aspirin provides a second hydrolysis site such that the acyl nitroso intermediate, which is likely to further hydrolyze to produce HNO and a carboxylate, may be either the salicylate (pathway A; **9a**) or acetylsalicylate (pathway B; **9b**) derivative. In either case, the products would be salicylate, HNO and isopropanol (from decomposition of **10**).

Alternatively, IPA/NO-aspirin (**3**) decomposition may be initiated by hydrolysis of one of the two ester bonds (Scheme 4). Cleavage of the acetyl bond (pathway A) would produce IPA/NO-salicylate (**7**), which could undergo further decomposition to form salicylate and

the O^2-hydroxymethyl-diazeniumdiolate. Spontaneous release of formaldehyde would give the free diazeniumdiolate, which can then decompose by Scheme 1. Conversely, initial cleavage of the prodrug (pathway B) would produce aspirin and the O^2-hydroxymethyl-diazeniumdiolate. Again, regardless of the pathway, the products will include salicylate, HNO and isopropanol, but isopropylamine and NO may also be formed. Scheme 3 is not accessible for the secondary amine prodrug DEA/NO-aspirin nor is the HNO donating pathway in Scheme 1, thus the expected products are salicylate, NO and diethylamine.

Of the many intermediates proposed in Schemes 3 and 4, those that may be both diagnostic and long-lived enough to be detected are aspirin in pathway B of both Schemes 3 and 4, NONO-salicylate (**7** or **8**) in pathway A of Scheme 4 and the free diazeniumdiolate in Scheme 4. Spectrophotometric, NMR and HPLC analyses were thus performed to assist with mechanistic assignment.

O^2-Derivatization stabilizes diazeniumdiolates, allowing for purification by column chromatography and increasing stability during storage, especially for primary amine adducts.[39] O^2-Protection also leads to a shift in the diazeniumdiolate absorption maximum from 250 to ~240 nm. For the new aspirin prodrugs, the rates of spontaneous hydrolysis as determined by loss of this peak/shoulder (Figures 1A and B) are significantly longer ($t_{½}$ of 7.5 and ~36 h for IPA/NO-aspirin and DEA/NO-aspirin, respectively, at pH 7.4 and 37°C) than for the parent diazeniumdiolates or acetoxymethyl derivatives (compare to 5.7 and 2.5 min for IPA/NO and DEA/NO[29], and 41 min for IPA/NO-AcOM[39]).

The final spectrum in Figure 1A corresponds to that of salicylate (λ_{max} of 238 and 295 nm). Importantly, the presence of a clear isosbestic point indicates negligible accumulation of aspirin (λ_{max} at 267 nm). Spontaneous hydrolysis of aspirin to salicylate (Figure 1C) at pH 7.4 occurs with a nearly threefold slower rate constant than IPA/NO-aspirin decomposition. Elevated pH accelerates the hydrolysis of both aspirin and IPA/NO-aspirin without leading to significant spectral changes from those in Figures 1A and C (data not shown). The differences in the rates of these processes however are even more pronounced ($(1.6 \pm 0.5) \times 10^{-4}$ s^{-1} and $(3.5 \pm 0.8) \times 10^{-3}$ s^{-1}, respectively at pH 10). These data therefore suggest that pathways 3-B and 4-B can be eliminated as major components of the decomposition mechanism of IPA/NO-aspirin, due to lower stability of the acetyl bond compared to the prodrug ester linker. Furthermore, that accumulation of free IPA/NO was not observed at pH 10, where the rate of decomposition (4.1×10^{-4} s^{-1}) is slower than that of IPA/NO-aspirin, also eliminates pathway 4-A. Thus, as with the acetoxymethyl derivative, IPA/NO-aspirin is suggested to decompose by amine deprotonation followed by pathway 3-A.

Analysis by NMR of the hydrolysis products of IPA/NO-aspirin at pH 10 (Figure S1) revealed significant accumulation of isopropanol (δ 1.18 [d, $(CH_3)_2$]), acetate (δ 1.91 [s, CH_3]), formaldehyde (δ 4.86 [s, CH_2]) and salicylate (δ 6.89-6.92, 7.39-7.42, 7.72-7.74). Notably, the acetyl group of aspirin was not observed (δ 2.33 (s, CH_3)). Isopropylamine (δ 1.07 [d, $(CH_3)_2$]) was also not detected, indicating that under these conditions, the NO-donating pathway in Scheme 1 was not appreciable, as would be expected even if pathways 4-A or 4-B were significant.

The spectral changes observed during decomposition of IPA/NO-aspirin and DEA/NO-aspirin are similar (Figures 1A,B), but a more pronounced initial shoulder near 275 nm may suggest early formation of aspirin from decomposition of DEA/NO-aspirin. Since the rate of hydrolysis of DEA/NO-aspirin is slower than that of aspirin by twofold, both pathways in Scheme 4 are kinetically viable.

Given the potential for NONO-salicylate (**7** or **8**) formation by pathway 4-A, the IPA/NO- and DEA/NO-salicylate derivatives were synthesized in a similar manner as shown in Scheme 3 and were found to have unique maxima at 306 nm. Their faster rates of decomposition (7.0×10^{-5} and 3.1×10^{-5} s^{-1}) indicate that early rate-limiting steps inhibit NONO-salicylate accumulation as useful to discriminate between potential pathways for the aspirin derivatives.

At pH 10, unlike for IPA/NO-aspirin (data not shown), decomposition of DEA/NO-aspirin produces observable intermediates. The peak near 275 nm in the initial spectrum suggests the presence of aspirin (Figure 1D). With time, this peak shifts to ~295 nm, indicating cleavage to salicylate (Figure 1E). Additionally, an initial growth of intensity near 250 nm suggests production of DEA/NO ($(4.5 \pm 0.6) \times 10^{-5}$ s^{-1}) (Figure 1D). Together, these data support spontaneous hydrolysis of DEA/NO-aspirin through pathway 4-B.

DEA/NO-aspirin hydrolysis products were examined by NMR spectroscopy at pH 10 in a similar manner as described for IPA/NO-aspirin. Formation of DEA/NO (2.99 and 0.94 ppm) was evident as early as 10 min (Figure S2). With time, DEA/NO aspirin decreased while that of a product (4.17, 3.72, 1.39, 1.27, and 1.12 ppm) increased, further reinforcing the generation of free DEA/NO. Hydrolysis of DEA/NO-aspirin was not complete as late as 92 h, evident from small observable peaks of the linker OCH_2O (6.13 ppm) and the acetyl group (2.40 ppm). Moreover, formation of DEA/NO-salicylate, free aspirin or the end product salicylate could not be firmly established due to overlapping aromatic peaks, which complicated assignment.

Scheme 4 can also be considered for both prodrugs in the presence of esterases. Addition of 2% guinea pig serum reduced the half-lives to 18 and 13 min, respectively for IPA/NO-aspirin and DEA/NO-aspirin (Figure 2). Additionally, the spectra differed significantly from those in Figure 1, with two processes evident. A new peak rapidly appeared at 306 nm with first-order rate constants of 0.035 ± 0.009 and 0.027 ± 0.006 s^{-1}, respectively (Figure 2A,B), and the slow first-order loss of the characteristic peak at 241 nm ($k_2 = (6.5 \pm 0.12) \times 10^{-4}$ and $(1.1 \pm 0.6) \times 10^{-3}$ s^{-1}, respectively) was accompanied by shifting of the 306 nm peak to 295 nm (Figure 2C,D).

The rate of hydrolysis of aspirin in the presence of guinea pig serum (Figure 2E) was found to be slower than either observed process ($(4.7 \pm 0.17) \times 10^{-4}$ s^{-1}), suggesting that aspirin should accumulate if formed. Similarly, if produced during the faster first step, free diazeniumdiolate should be observable spectrally, but a peak shift from 241 to 250 nm was not apparent. Furthermore, the intermediate spectra corresponded well to that of the NONO-salicylate derivatives, providing convincing evidence that esterase-mediated decomposition of the NONO-aspirin prodrugs proceeds primarily by pathway 4-A. Additionally, modeling using the kinetic data from Figure 2 and the rate constants for free diazeniumdiolate decomposition verified that accumulation of IPA/NO or DEA/NO by pathway 4-A would be insufficient at any time point to be observed spectrophotometrically (data not shown).

As additional confirmation, the species produced in the presence of guinea pig serum were monitored temporally by HPLC with UV detection (Figure 3). The initial chromatograms showed primarily the NONO-aspirin prodrugs (**3** and **6**), with traces of both aspirin and the NONO-salicylate derivatives (**7** and **8**). At 5 min, complete conversion to **7** or **8** was apparent. At 40 min, significant accumulation of free salicylate occurred from cleavage of **8**, while **7** provided to be more stable toward hydrolysis. The products and timing are consistent with the spectrophotometric analysis in Figure 2, thus providing further support of esterase-mediated decomposition by pathway 4-A.

The effect of FBS on the decomposition of IPA/NO-aspirin (Figure 2F) was also examined as it is commonly added to cell culture media. Interestingly, the rate constant (2.7×10^{-5} s^{-1}) was comparable to that in the absence of serum, but the slow appearance of a 306 nm peak and the subsequent shift to 295 nm suggested that esterase-mediated cleavage was occurring. This suggests that effective cleavage of the ester bonds of NONO-aspirin derivatives may require specific esterases.

NO and HNO release from NONO-aspirin prodrugs

Although there are many methods to directly or indirectly measure NO, detection of HNO is typically indirect and qualitative, in part due to metastability through an irreversible dimerization pathway (producing N_2O and water (8×10^6 M^{-1} s^{-1})[42]. We have designed and used a multi-step protocol in our prior analysis of IPA/NO[43] and IPA/NO-AcOM[39] and utilized similar methods here.

Reductive nitrosylation of ferric compounds such as metMb to the corresponding ferrous nitrosyl complex (MbNO) is often used to provide spectral verification of HNO production. For minute scale donors such as Angeli's salt and IPA/NO, aerated conditions allow this assay to discriminate between NO and HNO production due to the relative instability of the ferric compared to the ferrous nitrosyl complex of myoglobin. For longer-lived donors of HNO, the rate of autoxidation of MbNO back to metMb (2×10^{-4} s^{-1})[44] reduces the utility of this assay. Since performing this assay under deaerated conditions introduces other complicating factors, here, we substituted oxymyoglobin (MbO_2) for metMb. Although both NO (4×10^7 $M^{-1}s^{-1}$)[45, 46] and HNO (1×10^7 $M^{-1}s^{-1}$)[47] react with MbO_2 to produce metMb, addition of GSH (1 mM), which reacts facilely (2×10^6 M^{-1} s^{-1})[47] with HNO but not appreciably with NO,[48] provides specificity to the assay. Since autoxidation of MbO_2 ($k_{obs} = 1.2 \times 10^{-5}$ s^{-1}; data not shown) can become significant during the long decomposition times of the prodrugs in the absence of esterases, an excess of each prodrug was used to achieve higher reaction rates.

Both IPA/NO-aspirin and DEA/NO-aspirin converted MbO_2 to metMb (Figure 4A-D), and the calculated rate constants were similar to those determined for prodrug decomposition (respectively for IPA/NO-aspirin and DEA/NO-aspirin mediated formation of metMb, 9.8×10^{-5} and 3.3×10^{-5} s^{-1} in the absence of serum and 4.8×10^{-4} and 7.4×10^{-4} s^{-1} in the presence of serum). Addition of GSH only quenched metMb formation for IPA/NO-aspirin. In the absence of serum (Figure 4A), formation of metMb ($k_{obs} = 4.3 \times 10^{-5}$ s^{-1}) was reduced to a similar rate as that mediated by GSH alone[49] ($k_{obs} = 4.8 \times 10^{-5}$ s^{-1}, data now shown), suggesting that HNO is the primary product under these conditions. In contrast, less efficient scavenging by GSH was observed in the presence of serum (Figure 4C), indicating that NO production may be significant. These results are consistent with the higher yield of HNO expected from spontaneous hydrolysis via amine deprotonation (pathway 3-A) compared to ester cleavage to release free IPA/NO (pathway 4-A), which is a dual donor of HNO and NO at pH 7.4.

In the presence of an oxidant such as ferricyanide, detection methods for NO can be used to indirectly indicate formation of HNO.[50] The slow rate of spontaneous hydrolysis impedes such analysis, and therefore only the maximum current intensities observed with an NO-specific electrode during decomposition of the prodrugs in the presence of guinea pig serum are shown. For IPA/NO-aspirin (Figure 5A), the decrease in maximum signal intensity as the pH is elevated from 6 is rescued by addition of ferricyanide, indicating a successive increase in the relative yield of HNO at the expense of NO. That this profile is similar to that for IPA/NO[33] further supports cleavage as in Scheme 4. In contrast, the signal maxima from DEA/NO-aspirin are relatively constant, as expected for an NO only donor. The decrease in

maximum signal for both IPA/NO-aspirin and DEA/NO-aspirin below pH 6 indicates reduced serum esterase activity.

Given the dependence of IPA/NO-aspirin decomposition on the presence of serum and the sensitivity to serum type, the question arises as to the mechanism of decomposition within human cells. Intracellular detection of NO and HNO is often achieved with fluorescent dyes such as diaminofluorescein (DAF).[51] Although typically non-specific toward HNO and NO, a higher relative signal is produced by HNO compared to NO.[52] Figure 6 shows the temporal profiles of fluorescent signal upon exposure of A549 cells loaded with the cell permeable dye DAF-FM-2DA to IPA/NO-aspirin, DEA/NO-aspirin and their constituent components.

Although the ionic diazeniumdiolate precursors decompose relatively rapidly, HNO and NO must then diffuse into the cells to react with the fluorophore. The higher signal intensities for the prodrugs thus indicate significant cellular uptake, allowing HNO and NO to be produced in close proximity to the reporter molecule, which will reduce cellular scavenging. Although NO may be produced directly from IPA/NO-based donors or HNO may be converted to NO by intracellular oxidants such as Cu,Zn SOD, the higher signals for IPA/NO and IPA/NO-aspirin relative to DEA/NO and DEA/NO-aspirin respectively indicate significant reactivity with HNO in the former cases. The only slightly slower rates of the signal increase for the prodrugs compared to the parent donors suggests that esterase-mediated cleavage of the prodrugs was significant within the cells.

Effect of NONO-aspirin prodrugs on ulcerogenicity

One of the most common side effects of aspirin use is gastrointestinal ulceration. NO releasing NSAIDs have previously been shown to protect the stomach lining,[27] but the effect of HNO releasing NSAIDs is not known. To establish the safety profile of the new prodrugs, the ulcerogenicity was measured by scoring the number and size of ulcerations. Both IPA/NO-aspirin (3.3 ± 3) and DEA/NO-aspirin (0) (Figure 7) showed a substantially lower ulcer index as compared to aspirin (57.4 ± 3.1; see for example reference 27 for images of aspirin-mediated ulcerations).

At highly acidic pHs such as that of the stomach, ionic diazeniumdiolates decompose rapidly, and potentially accessible HNO-producing pathways are suppressed in favor of NO production (Scheme 1). That O^2-derivatized diazeniumdiolates are stable under acidic conditions (data not shown for the aspirin derivatives) may allow for significant absorption by the stomach lining before cleavage. The reduced ulcerogenicity of IPA/NO-aspirin and DEA/NO-aspirin may then be due to inhibition of an aspirin-mediated effect either by structural derivatization, by decomposition to salicylate, by enhanced clearance or may be due to the prodrug itself functioning as a selective inhibitor of COX-2. Ulcerogenicity may also be affected by the presence of NO or HNO, if cleavage does occur in the gastrointestinal system. O^2-Derivatization may thus facilitate intracellular delivery and bioactivation as well as preserve pathways that lead to HNO rather than NO production.

Anti-inflammatory properties of NONO-aspirin prodrugs compared to aspirin

To verify whether IPA/NO-aspirin and DEA/NO-aspirin retain the anti-inflammatory properties of the parent NSAID, they were orally administered to rats with paw edema induced by carrageenan.[27] Aspirin (ID_{50} = 129 mg/kg) and IPA/NO-aspirin (ID_{50} = 121 mg/kg) were found to be comparably potent while DEA/NO-aspirin (ID_{50} = 169 mg/kg) had slightly lower efficacy.

Administration of aspirin has previously been shown to increase COX-2 expression,[53] likely as a compensatory response to reduced prostaglandin levels due to irreversible inhibition.

Here, the effects of the prodrugs on COX-2 activity were examined in A549 cells, which are known to express high levels of COX-2.[54] PGE_2 levels, which are a direct measure of COX-2 activity,[9, 55] were decreased most significantly by IPA/NO-aspirin (Figure 8). These data support the conclusion from Figure 6 that the prodrugs induce more potent effects, likely due to improved cellular uptake and delivery.

The enhanced impact of IPA/NO-aspirin compared to DEA/NO-aspirin is also consistent with the formation of unique reactive species. If HNO is involved directly in COX-2 inhibition, the most likely targets are the ferric heme prosthetic group or cysteine residues.[47, 56, 57] Covalent modification of critical cysteine residues by HNO to produce a stable sulfinamide ($RS(O)NH_2$) derivative has previously been shown to inhibit enzymes such as aldehyde dehydrogenase and glyceraldehyde 3-phosphate dehydrogenase (GAPDH).[58-60] Although the cysteine residues of COX-2[57] may similarly be affected by HNO, the mechanism of inhibition by IPA/NO-aspirin requires further investigation.

Effect of NONO-aspirin prodrugs on cell viability

Intake of NSAIDs has been shown to improve the efficacy of chemotherapy for certain tumors and even to reduce the risk of developing a variety of cancers.[61, 62] Tumor cells produce enhanced levels of PGE_2,[63] which play an important role in cancer progression[64-67] by increasing metastasis, cell proliferation[68] and angiogenesis[69-71] and reducing immune response[72] and apoptosis.[71] Increased levels of COX-2 are also associated with chronic inflammation and result in more aggressive phenotypes and poor patient outcome.[73, 74] The role of NO in cancer has been investigated extensively[75] while HNO donors has very recently been shown to inhibit breast[36] and neuroblastoma[76] cancer proliferation in mouse xenografts as well as in culture through increased apoptosis[36]. The data in Figure 8 thus suggest that HNO-donating NONO-NSAIDs may have utility as anti-cancer agents. Preliminary analysis of this functionality was obtained here from cell proliferation data.

The cytotoxicity of both aspirin and ionic diazeniumdiolates in various cancer cells lines is low (IC_{50} > 1 mM).[43, 77] In contrast, the cytotoxicity toward A549 cells of the two prodrugs after 48 h of treatment was determined by the standard MTT assay to be significantly higher (Figure 9A; IC_{50} of ~90 and 135 μM for IPA/NO-aspirin and DEA/NO-aspirin, respectively). That these compounds were not appreciably toxic to normal endothelial cells (HUVECs; Figure 9B, no effect on viability up to 100 μM) suggests a cancer–specific sensitivity that is promising for chemotherapy or chemoprevention.

Effect of NONO-aspirin prodrugs on GAPDH activity

Given the hypoxic micro-environments of many solid tumors,[78] cancer cells have a higher dependence on glycolysis than normal cells.[79, 80] Thus, inhibition of the glycolytic protein GAPDH is a promising means to selectively target tumor cells.[81] GAPDH is also involved in initiation of apoptosis, DNA repair, endocytosis, nuclear membrane assembly, cytoskeletal dynamics.[82] The critical thiol of GAPDH can be inhibited by HNO donors,[58-60] and this effect has been demonstrated previously to inhibit breast cancer growth.[36] Here, that the inhibition of GAPDH activity was highest for IPA/NO-aspirin (Figure 10) further supports a mechanism to produce HNO and may partially be responsible for the higher cytotoxicity of IPA/NO-aspirin compared to DEA/NO-aspirin toward A549 cells (Figure 9).

Effect of IPA/NO-aspirin on contractility and relaxation in isolated adult ventricular mouse myocytes

Although low daily doses of aspirin can be cardioprotective,[83] chronic use of NSAIDs, particularly COXIBs, is also associated with an increased risk of myocardial infarction.[84] Both HNO and NO donors have also been demonstrated to protect against ischemia-

reperfusion injury.[85] Additionally, enhanced contractility is an important pharmacological effect of HNO donors and is unique from NO donors.[35] Here, the impact of IPA/NO-aspirin on mechanical function and whole calcium transients in isolated murine myocytes was investigated as the final indicator of HNO production. In this assay, 500 μM IPA/NO-aspirin was used to produce a significant flux of HNO, given the long half-life of IPA/NO-aspirin and the short stability of isolated murine myocytes (20-30 min). When isolated murine myocytes were superfused with IPA/NO-aspirin, a significant increase in sarcomere shortening, which is an index of myocyte contractility, was observed (+201 ± 18% from control, n =12, $p < 0.0001$; Figure 11A and C). This change was paralleled by a significant rise in the whole calcium transient (24 ± 6%, $p < 0.001$, Figure 11B and D) and a reduction of the time required for the myocyte to fully relax, as indexed by the time of half-relaxation from peak shortening (−17 ± 3%, $p < 0.005$) (Figure 11E). Thus, in analogy to previous evidence[86] obtained with the prototypical HNO donor Angeli's salt, IPA/NO-aspirin enhanced the function of adult ventricular myocytes isolated from adult mouse hearts. This confirms that in the heart, HNO donors are positive inotropic/lusitropic agents and increase cardiomyocyte Ca^{2+} transients.[87, 88]

Conclusions

Both IPA/NO and DEA/NO can be readily derivatized to form NSAID adducts, which increases stability and improves purifiability. While NO releasing NSAIDs have been reported previously, this is the first example of an HNO donating NSAID. Such adducts retain the anti-inflammatory properties of aspirin while reducing gastric toxicity. Additionally, the mechanisms of decomposition, the donor profiles and the nitrogen oxide-induced effects are all consistent with other O^2-derivatized diazeniumdiolates. The prodrugs lead to enhanced intracellular delivery of HNO and NO, which may be beneficial pharmacologically, given the variety of cellular scavenging mechanisms for nitrogen oxides. Of particular interest is the observation of enhanced cytotoxicity compared to the individual components toward adenocarcinoma but not normal endothelial cells, suggesting a potential for use in cancer treatment or prevention. The mechanistic basis for this selectivity is currently under investigation, but likely involves a decrease of the Warburg effect as well as inhibition of COX activity. In summary, long-lived HNO and NO donating aspirin prodrugs may have wide therapeutic applicability as anti-inflammatory, anticancer and cardioprotective agents.

Experimental Section

Unless otherwise noted, chemicals were purchased from Sigma-Aldrich and were used without further purification. IPA/NO and DEA/NO were synthesized according to previously published procedures.[89] Concentrations of NONOate stock solutions (>10 mM), prepared in 10 mM NaOH and stored at –20°C, were determined directly prior to use from the extinction coefficients at 250 nm (ε of 8,000 $M^{-1}cm^{-1}$).[29] Stock solutions other than of nitrogen oxide donors were prepared fresh daily at 100× in MilliQ or Barnstead Nanopure Diamond filtered H_2O, unless specified. Typically, the assay buffer consisted of the metal chelator diethylenetriaminepentaacetic acid (DTPA, 50 μM) in calcium- and magnesium-free Dulbecco's phosphate-buffered saline (PBS, pH 7.4). By sequestering contaminating metals, addition of DTPA quenched the oxidation of HNO to NO.[90] All reactions were performed at 37°C except those measured with the NO-specific electrode, which were run at room temperature. Thin layer chromatography (TLC) was carried out using Analtech silica gel GF (250 micron) glass-backed plates. Eluted plates were visualized at 254 nm. Flash chromatography was performed using the indicated solvent system on Silica Gel 60 (230-450 mesh size; Alfa Aesar). Compound purity was analyzed using HPLC analysis (Agilent 1100 series diode array detector) and high resolution mass spectrometry (JEOL

HX110A spectrometer). Compounds of >95% were used for subsequent experiments (see the Supporting Information).

Instrumentation—UV-visible spectroscopy was performed with an Agilent Hewlett-Packard 8453 diode-array spectrophotometer equipped with an Agilent 89090A thermostat. PerkinElmer HTS 7000 or BioTek Synergy 2 microplate readers were also utilized for absorbance and fluorescence measurements. Electrochemical detection was accomplished with a World Precision Instruments Apollo 4000 system with NO, O_2 and H_2O_2 sensitive electrodes. A PerkinElmer HTS 7000 plate reader was utilized for absorbance and fluorescence measurements. Solution pH was determined by use of a ThermoElectron Orion 420A+ pH meter. ^{1}H and ^{13}C NMR spectra were acquired using a Bruker AM-500 spectrometer (500 MHz). Positive ion electrospray ionization mass spectra were obtained with a JEOL HX110A spectrometer). CHN microanalyses were performed at Columbia Analytical Services (Tucson, AZ). HPLC with UV detection was carried out using an Agilent 1100 series solvent delivery system coupled with an Agilent 1100 series diode array detector.

O^2-(Methylthiomethyl)-1-(N-isopropylamino)diazen-1-ium-1,2-diolate (1)— Chloromethyl methyl sulfide (1.93 mL, 23.4 mmol) was added to a slurry solution of Na_2CO_3 (1.24 g, 11.7 mmol) in DMF (50 mL) at room temperature. Following 2 min of stirring IPA/NO (3.29 g, 23.4 mmol) was added, and stirring was continued for 3 h. The reaction was quenched by addition of ethyl acetate (70 mL), and the solution was then filtered and subsequently washed with 10% NaCl solution (5 × 40 mL). The organic layer was then dried over Na_2SO_4 and evaporated to obtain the crude product, which was further purified by column chromatography using ethyl acetate/hexane (1:4 v/v) to obtain a light yellow oil (780 mg, 19%). ^{1}H NMR ($CDCl_3$): δ 1.22 [d, J = 6.5 Hz, 6H, CH_3], 2.28 [s, 3H, CH_3], 4.06 [septet, J = 6.5Hz, 1H, CH], 5.24 [s, 2H, CH_2], 6.05 [b, 1H, NH]. ^{13}C NMR ($CDCl_3$): δ 14.70 [CH_3], 19.96 [SCH_3], 48.78 [CH], 78.0 [OCH_2S].MS (HRMS) calculated $M+Na^+$ 202.0621, found 202.0619.

O^2-(Chloromethyl)-1-(N-isopropylamino)diazen-1-ium-1,2-diolate (2)—A solution of **1** (0.761 g, 4.25 mmol) dissolved in dichloromethane (17 mL) was cooled to −78°C, and sulfuryl chloride (4.67 mL of 1.0 M solution in CH_2Cl_2, 4.67 mmol) was added drop-wise with stirring. The reaction mixture was brought to room temperature, and completion of the reaction was monitored by TLC. After 3 h, the reaction mixture was filtered and evaporated to yield a yellow oil that was then used immediately without further purification. ^{1}H NMR ($CDCl_3$): δ 1.22 [d, J = 6.5 Hz, 6H, CH_3], 4.02 [septet, J = 6.5 Hz, 1H, CH], 5.8 [s, 2H, CH_2], 6.23 [b, 1H, NH]. ^{13}C NMR ($CDCl_3$): δ 20.39 [CH_3], 49.37 [CH], 79.25 [CH_2Cl].

O^2-(Acetylsalicyloyloxymethyl)-1-(N-isopropylamino)-diazen-1-ium-1,2-diolate (IPA/NO-aspirin) (3)—Aspirin (765 mg, 4.25 mmol) was dissolved in DMSO (5 mL), triethylamine (0.592 mL, 4.25 mmol) was added, and the solution was stirred for 50 min at room temperature. A solution of **2** in DMSO (5 mL) was then added drop-wise. The reaction mixture was stirred for 15 h then quenched with ethyl acetate (40 mL). The organic layer was washed with a saturated $NaHCO_3$ solution (5 × 40 mL), dried over Na_2SO_4 and then evaporated to obtain the crude product. Further purification was performed by silica gel column chromatography using ethyl acetate/hexane (1:4 v/v) to obtain IPA/NO-aspirin (460 mg, 38%) as a viscous clear oil. ^{1}H NMR ($CDCl_3$): δ 1.16 [d, J = 6.5 Hz, 6H, $(CH_3)_2$], 2.33 (s, 3H, $COCH_3$), 3.98 (septet, J = 6.5 Hz, 1H, CH), 5.94 (s, 2H, OCH_2O), 6.16 (b, 1H, NH), 7.1 (dd, J = 8 Hz, 1 Hz, phenyl H-3), 7.30 (td, J = 3 Hz, 1 Hz, phenyl H-5), 7.60 (td, J = 3.5 Hz, 1.5 Hz, phenyl H-4), 8.04 (dd, J = 8 Hz, 1.5 Hz, phenyl H-6). ^{13}C NMR ($CDCl_3$): δ 20.87 ($CO\underline{C}H_3$), 21.4 [$(CH_3)_2$], 49.65 (CH), 88.16 (CH_2), 122.59 (aromatic C1), 124.34

(aromatic C3), 126.50 (aromatic C5), 132.5 (aromatic C6), 135.01 (aromatic C4), 151.47 (aromatic C2), 163.17 (C=O), 170.04 (O<u>C</u>=OCH$_3$) Elemental analysis ($C_{13}H_{17}N_3O_6$): C = 50.16; H = 5.50; N = 13.50 (theoretical), C = 49.92; H = 5.42; N = 13.42 (experimental). MS (LRMS): 334.1 (M+Na$^+$ peak). Mass spec (HRMS): calculated M+H$^+$ 312.11901, Found 312.11908.

O^2-(Methylthiomethyl)-1-(N,N-diethylamino)diazen-1-ium-1,2-diolate (4)— Chloromethyl methyl sulfide (1.86 mL, 22.5 mmol) was added to a mixture of Na_2CO_3 (2.39 g, 22.5 mmol) and DMF (50 mL), and the reaction solution was stirred at room temperature for 5 min. DEA/NO (3.50 g, 22.5 mmol) was then added, and stirring was continued for 3 h. The reaction mixture was quenched by addition of 70 mL ethyl acetate and filtered. The organic layer was washed with 10% NaCl solution (5 × 40 mL), dried over Na_2SO_4, and evaporated to obtain the crude product, which was further purified by silica gel column chromatography using ethyl acetate/hexane (1:4 v/v) to give a light yellow oil (2.61 g, 60%). ^{1}H NMR ($CDCl_3$): δ 1.05 [t, *J* = 7 Hz, 6H, CH_3], 2.21 [s, 3H, SCH_3], 3.09 [q, *J* = 7 Hz, CH_2], 5.23 [s, 2H, OCH_2]. ^{13}C NMR ($CDCl_3$): δ 11.47 [$(CH_3)_2$], 15.11 [CH_3], 48.46 [$(CH_2)_2$], 78.32 [OCH_2S]. Mass spec (HRMS): calculated M+H$^+$ 194.0958, found 194.0957.

O^2-(Chloromethyl)-1-(N,N-diethylamino)diazen-1-ium-1,2-diolate (5)—A solution of **4** (2.10 g, 11.5 mmol) was prepared in dichloromethane (120 mL), and the reaction mixture was cooled to –78°C. Sulfuryl chloride (1.12 mL, 13.8 mmol) was added slowly using a dropping funnel, and the reaction mixture was brought to room temperature. Reaction progress was monitored by TLC. The reaction mixture was washed with water, dried over $MgSO_4$, filtered and evaporated, and then used immediately without further purification. ^{1}H NMR (CD_3CN): δ 1.10 [t, *J* = 7 Hz, 6H, CH_3], 3.30 [q, *J* = 7 Hz, 4H, CH_2], 5.97 [s, 2H, CH_2]. ^{13}C NMR (CD_3CN): δ 11.67 [CH_3], 48.52 [CH_2], 80.94 [OCH_2Cl].

O^2-(Acetylsalicyloyloxymethyl)-1-(N,N-diethylamino)-diazen-1-ium-1,2-diolate (DEA/NO-aspirin) (6)—Triethylamine (1.46 ml, 10.4 mmol) was added to a solution of acetylsalicylic acid (1.87 g, 10.4 mmol) in DMSO (20 mL), and the reaction mixture was stirred for 30 min at room temperature. A solution of **5** (1.88 g, 10.4 mmol) dissolved in DMSO (20 mL) was added dropwise to the reaction mixture. After 24 h, the reaction was quenched with ethyl acetate (70 mL). The organic layer was washed with 10% NaCl solution five times and evaporated to give the crude product, which was purified by silica gel column chromatography using ethyl acetate/hexane (3:7 v/v) to obtain a viscous yellow oil (2.2 g, 65%). ^{1}H NMR (500 MHz, $CDCl_3$): δ 1.08 [t, *J* = 4.5 Hz, 6H, $(CH_3)_2$], 2.33 (s, 3H, $COCH_3$), 3.2(q, *J* = 7 Hz, 4H, CH_2), 5.995 (s, 2H, OCH_2O), 7.09 (dd, *J* = 1, 8 Hz, phenyl H-3), 7.3 (td, *J* = 1, 7.5 Hz, phenyl H-5), 7.6 (td, *J* = 1, 8 Hz, phenyl H-4), 8.03 (dd, *J* = 1, 8 Hz, phenyl H-6). ^{13}C NMR (500 MHz, $CDCl_3$): δ 11.45 [$(CH_3)_2$], 20.99 ($COCH_3$), 48.00 [$(CH_3)_2$], 87.90 (CH_2), 122.07 (aromatic C1), 123.98 (aromatic C3), 126.0 (aromatic C5), 131.59 (aromatic C6), 134.521 (aromatic C4), 151.119 (aromatic C2), 162.52 (C=O), 169.55 (OC=OCH$_3$). Elemental analysis ($C_{13}H_{17}N_3O_6$): C = 51.69; H = 5.89; N = 12.92 (theoretical), C = 51.49; H = 5.13; N = 12.73 (experimental), MS (LRMS): 348.1 (M+Na$^+$ peak). Mass spec (HRMS): calculated M+H$^+$ 326.13466, Found 326.13470.

O^2-(2-hydroxybenzoyloxymethyl)-1-(N-isopropylamino)-diazen-1-ium-1,2-diolate (IPA/NO-salicylate) (7)—Triethylamine (388 μL 2.78 mmol) was added to a solution of salicylic acid (0.385 g, 2.78 mmol) in DMSO (10 mL), and the reaction mixture was stirred for 30 min at room temperature. An equimolar solution of **2** in DMSO (10 mL) was added dropwise to the reaction mixture. After 24 h, the reaction was quenched with ethyl acetate (70 mL). The organic layer was washed with 10% NaCl solution five times and evaporated to give the crude product, which was purified by silica gel column

chromatography using CH_2Cl_2/hexane (1:1 v/v) to obtain a viscous oil (112 mg, 14.9%). ^{1}H NMR ($CDCl_3$): δ 1.16 [d, J = 6.5 Hz, 6H, $(CH_3)_2$], 3.95 (septet, J = 6.5 Hz, 1H, CH), 5.99 (s, 2H, OCH_2O), 6.16 (b,1H, NH) 6.77-6.91 (m, 1H, aromatic), 6.97 (d, 1H, J = 8.4 Hz, aromatic), 7.46 (dd, 1H, J = 4.5, 11.1 Hz, aromatic), 7.84 (dd, 1H, J = 1.5, 8 Hz, aromatic), 10.4 (s, 1H, OH). ^{13}C NMR ($CDCl_3$): δ 20.37 [$(CH_3)_2$], 49.27 (CHN), 87.51 (CH_2O), 111.44 (aromatic), 117.68 (aromatic), 119.33 (aromatic), 130.12 (aromatic), 136.44 (aromatic), 162.01 (aromatic C), 168.63 (C=O). MS (HRMS): calculated M+Na^+ 292.0904, found 292.0905.

O^2-(2-hydroxybenzoyloxymethyl)-1-(N,N-diethylamino)-diazen-1-ium-1,2-diolate (DEA/NO-salicylate) (8)—Triethylamine (0.69 mL, 4.9 mmol) was added to a solution of salicylic acid (0.66 g, 4.1 mmol) in DMSO (5 mL), and the reaction mixture was stirred for 30 min at room temperature. An equimolar solution of **5** in DMSO (5 mL) was added dropwise to the reaction mixture. After 24 h, the reaction was quenched with ethyl acetate (70 mL). The organic layer was washed with 10% NaCl solution five times and evaporated to give the crude product, which was purified by silica gel column chromatography using CH_2Cl_2/hexane (1:1 v/v) to obtain a viscous oil (85.3 mg, 7%). ^{1}H NMR ($CDCl_3$): δ 1.08 [t, J = 7 Hz, 6H, $(CH_3)_2$], 3.19 (q, J = 7 Hz, 4H, CH_2), 6.06 (s, 2H, OCH_2O), 6.84 (ddd, J = 1.1, 8.25, 7.2 Hz, aromatic), 6.96 (dd, J = 1.1, 8.45Hz, aromatic), 7.46 (ddd, J = 1.75, 7.2 8.75 Hz, aromatic), 7.84 (dd, J = 1.75, 8 Hz, aromatic), 10.4 (s, 1H, OH). ^{13}C NMR ($CDCl_3$): δ 11.4 [$(CH_3)_2$], 48.13 [$(CH_3)_2$], 87.65 (CH_2), 111.47 (aromatic), 117.73 (aromatic), 119.35 (aromatic), 130.1 (aromatic), 136.47 (aromatic), 162.09 (aromatic), 168.63 (C=O). MS (HRMS): calculated M+Na^+ 306.1060, found 306.1056

Decomposition profiles and half-lives of NONO-aspirin prodrugs—The rate of NONO-aspirin prodrug decomposition in the presence or absence of 2% guinea pig serum was measured spectrophotometrically at 238 nm. The spectrophotometer was blanked with assay buffer ± guinea pig serum (20 μL/mL buffer), typically of pH 7.4 or 10 (adjusted prior to use by adding 1 M NaOH or HCl as necessary) and 37°C. A stock of NONO-aspirin derivative in DMSO (1000×, prepared by mass to 100 mM) was added to the assay buffer to initiate the reaction. With guinea pig serum, spectra were collected every second for 600 s then at intervals of 60 s for DEA/NO-aspirin and at 120 s for IPA/NO-aspirin. In the absence of serum, spectra were collected at 1800 s intervals. With fetal bovine serum (FBS; HyClone), 900 s intervals were used for IPA/NO-aspirin. Total scan times ranged from 2500 s to 62 h. Kinetic analysis was performed by fitting the data to an exponential decay ($A = \Delta A e^{-kt} + A_\infty$).

Organic products of hydrolysis of IPA/NO-aspirin (3-4 mg) at pH 10 and 37°C for 24 h were characterized by NMR spectroscopy in 40% w/w NaOD (Alfa Aesar) in D_2O (Cambridge Isotope). Water suppression was achieved by using the preset pulse sequence. Identification was verified by comparison with authentic standards.

The stability of the NONO-aspirins were evaluated in the presence of 2% guinea pig serum. In each case 0.1 M phosphate buffer (pH 7.4) with 50 μM DTPA was preheated to 37°C, and the reactions were initiated by the addition of either IPA/NO- or DEA/NO-aspirin to a final concentration of 100 μM. The reactions were monitored as a function of time by HPLC. Separations were carried out on a Phenomenex Luna C18 column, 3 μm, 150 × 2.1 mm, using a water and acetonitrile gradient containing 0.1% formic acid. Product identity was confirmed by co-elution with authentic standards.

Detection of HNO and NO—The methods described below for detection of HNO and NO were utilized in our prior analysis of IPA/NO[43] and IPA/NO-AcOM[39] and are described in more detail in reference 91.

Reaction of NO and HNO with oxymyoglobin—The spectrophotometer was blanked with assay buffer ± guinea pig serum (20 μL/mL buffer) at pH 7.4 and 37°C. Oxymyoglobin (MbO_2; 50 μM) (ε_{542} = 13.9 mM^{-1} cm^{-1}; ε_{580} = 14.4 mM^{-1} cm^{-1})[92] was exposed to IPA/NO-aspirin or DEA/NO-aspirin (50 or 250 μM) to form metmyoglobin (metMb; ε_{502} = 10.2 mM^{-1} cm^{-1}; ε_{630} = 3.9 mM^{-1} cm^{-1}).[92] Formation of HNO was further verified by inclusion of GSH,[47] which quenches HNO chemistry without interacting directly with low concentrations of NO[48]. Spectra were collected at 30-900 s intervals for 800 s to 6 h. The rate of autoxidation of MbO_2 was monitored at 600 s intervals for 12 h.

Electrochemical detection of NO and HNO—The NO electrode was stabilized in assay buffer of the desired pH containing 50 μM DTPA and 2% serum at room temperature. IPA/NO-aspirin or DEA/NO-aspirin were added to a final concentration of 100 μM (total DMSO volume ≤ 0.1%), and the maximum signal intensity was recorded. After the signal returned to baseline, the process was repeated to obtain triplicate measurements. Addition of 1 mM sodium ferricyanide, which oxidizes HNO to NO, allows for indirect measurement of HNO with this system.[50]

Cell culture—Human lung adenocarcinoma epithelial cells (A549; American Type Culture Collection, Manassas, VA) and human umbilical vascular endothelial cells (HUVECs; Cell Applications, Inc., San Diego, CA) were grown as monolayers in either RPMI 1640 media supplemented with 10% FBS, penicillin and streptomycin (50 U/mL; Life Technologies, Inc., Grand Island, NY) for A549 cells or endothelial growth medium (Cell Applications, Inc., San Diego, CA) for HUVECs at 37°C in 5% CO_2 and 80% relative humidity. Single cell suspensions were obtained by trypsinization (0.05% trypsin/EDTA), and cells were counted with a Beckman cell counter.

Intracellular release of NO and HNO—A549 cells were plated at 60,000 cells per well in a 96-well plate and grown for 4 h as above. A stock (100×) of 4-amino-5-methylamino-2', 7'-difluorofluorescein diacetate[93] (DAF-FM-2DA, Molecular Probes) in DMSO was diluted to a final concentration of 10 μM in PBS. The media was aspirated from each well, and the plate was washed once with PBS. The cells were then exposed to 100 μL of 10 μM DAF-FM-2DA for 75 min at 37°C and washed three times with PBS to remove excess dye. NONO-aspirin derivatives dissolved in DMSO (1000×) and ionic NONOates dissolved in 10 mM NaOH (1000×) were then added to achieve a final concentration of 10 μM. The increase in fluorescence intensity at 535 nm as a function of time was then measured following excitation at 485 nm.

Effect of NONO-aspirin prodrugs on PGE_2 levels—A549 cells were plated at 50,000 cells per well in a 96 well plate and grown for 12 h as above. Then, NONO-aspirin prodrugs (25 or 50 μM; DMSO ≤ 0.1%) were added, and the plate was incubated at 37°C for 24 h. The supernatant was then analyzed for prostaglandin E_2 (PGE_2) activity using a PGE_2 EIA kit (Cayman Cat No. 514010). A volume of 50 μL of the diluted sample was added to a 96-well plate followed by addition of 50 μL of both PGE_2 AChE tracer and PGE_2 monoclonal antibody. The samples were incubated overnight at 4°C. The plate was then washed five times (200 μL each) with wash buffer, and then Edman's reagent (200 μL per well) was added as described in the assay protocol. The absorbance at 450 nm was determined using a plate reader.

Effect of NONO-aspirin prodrugs on cell viability as determined with the standard colorimetric MTT assay—Cells were plated at 8,000-10,000 cells per well in a 96-well plate and grown overnight as above. The cells were then treated with different concentrations (0-200 μM) of the prodrugs for 48 h. After addition of 10 μL of a solution of

2 mg/mL of 3-(4,5-dimethylthiazol-2-yl)-2,5-diphenyltetrazolium bromide (MTT) to each well, the plate was incubated for 1 h at 37°C. The media was then removed, 100 μL DMSO was added to each well, and the absorbance was recorded at 550 nm using a BioTek Synergy 2 microplate reader.

Effect of NONO-aspirin prodrugs on GAPDH activity—Cells were plated at 30,000 cells per well in a 96-well plate grown overnight, and treated with 100 μM IPA/NO-aspirin or DEA/NO-aspirin for 1 h. For measurement of GAPDH activity, a KDalert™ GAPDH assay kit from Applied Biosystems (Cat #AM1639) was used. The cells were lysed by addition of 200 μL of KDalert lysis buffer to each well followed by incubation at 4°C for 20 min. Then, 2.5 μL of cell lysate was transferred to a clean 96 well plate, 97.5 μL of KDalert mastermix was added to each well, and fluorescence at 570 nm was measured after excitation at 540 nm.

Animal protocols—The anti-inflammatory and ulcer index assays described below were carried out using protocols approved by the Health Sciences Animal Welfare Committee at the University of Alberta. The protocols to evaluate mechanical function and whole Ca^{2+} transient were approved by the Animal Care and Use Committee of the Johns Hopkins University, and adhered with NIH public health service guidelines.

Effect of NONO-aspirin prodrugs on inflammation—The anti-inflammatory properties of the prodrugs were determined *in vivo* in a carrageenan induced rat paw edema assay model.[94] Sprague-Dawley rats weighing 160-180 g (n = 3) were orally administered with aspirin, IPA/NO-aspirin or DEA/NO-aspirin (0.8 mmol/kg) suspended in 1.2 mL of water containing 1% methyl cellulose. After 1 h, each group was injected with 100 μL of 1% carrageenan suspension in 0.9% NaCl solution in the right hind paw to induce inflammation. The volume of the injected paw was measured at 0 and 3 h using a UGO Basile 7141 Plethysmometer (series no. 43201). After 3 h, anti-inflammatory activity was calculated using the corresponding dose-response curves, as the dosage required to decrease the maximum inflammatory response (control group) by 50%. Animals in the control group received an equivalent volume of 1% methylcellulose solution.

Effect of NONO-aspirin prodrugs on ulcerogenicity—Stomach ulceration was evaluated *in vivo* using Sprague-Dawley rats (n = 3) according to published procedures.[95] Each rat was dosed (p. o.) with equimolar amounts (1.38 mmol/kg) of aspirin, IPA/NO-aspirin or DEA/NO-aspirin suspended in 1.2 mL of a 1% methylcellulose solution (vehicle) except control rats, which received vehicle. Food, but not water, was removed 24 h before administration of test compounds. At 6 h post-administration, the rats were euthanized in a CO_2 chamber, and their stomachs were removed and placed on ice. Ulceration was examined with a magnifying glass and scored based on their number and size (1 mm, rating of 1; 1-2 mm, rating of 2; and >2 mm, rating according to their length in millimeters).[27] The ulcer index (UI) for each compound was calculated by adding the total length (L, in mm) of individual ulcers in each stomach and averaging over the number of animals in each group (n = 4): $UI = (L_1+L_2+L_3+L_4)/4$.

Evaluation of the effects of IPA/NO-aspirin on mechanical function and whole Ca^{2+} transient in isolated adult murine myocytes—Wild type 2-4 month old mice were anesthetized with intraperitoneal sodium pentobarbital (100 mg/kg), and cardiomyocyte were isolated.[86, 96] Sarcomere shortening was determined by imaging the cells using field stimulation (0.5 Hz) in an inverted fluorescence microscope (Diaphot 200; Nikon, Inc). Sarcomere length was evaluated by real-time Fourier transform (IonOptix MyoCam, CCCD100M) and expressed as the time from peak shortening to 50% relaxation.

Calcium transient was measured by confocal laser scanning microscope (LSM510, Carl Zeiss) by loading myocytes with fluo-4/AM (Molecular Probes, 20 μM for 30 min). All measurements were carried out at room temperature.

Statistical analysis—All data are expressed as mean ± SD, and one-way ANOVA or t-test was applied to determine the significance of the difference between control and treatment groups.

Supplementary Material

Refer to Web version on PubMed Central for supplementary material.

Acknowledgments

This work is supported in part by a National Institutes of Health grant (R01-GM076247 to K.M.M), the Intramural Research Program of the National Institutes of Health, National Cancer Institute and Center for Cancer Research (D.A.W.) and by start-up funds from the Faculty of Pharmacy and Pharmaceutical Sciences at the University of Alberta (C.A.V.-M.).

Abbreviations

Angeli's salt	sodium trioxodinitrate
A549	human alveolar adenocarcinoma
CINOD	COX inhibiting nitric oxide donors
COX	cyclooxygenase
COXIB	selective inhibitors of COX-2
DAF-FM-2DA	4-amino-5-methylamino- 2',7'-difluorofluorescein diacetate
DEA/NO	sodium 1-(N,N-diethylamino)diazen-1-ium-1,2-diolate
DEA/NO-aspirin	O^2-(acetylsalicyloyloxymethyl)-1-(N,N-diethylamino)-diazen-1-ium-1,2-diolate
DTPA	diethylenetriaminepentaacetic acid
EDTA	ethylenediaminetetraacetic acid
GSH	glutathione
NO	nitroxyl
IPA/NO	sodium 1-(N-isopropylamino)diazen-1-ium-1,2-diolate
IPA/NO-AcOM	O^2-(acetoxymethyl)-1-(isopropylamino)diazen-1-ium-1,2-diolate
IPA/NO-aspirin	O^2-(acetylsalicyloyloxymethyl)-1-(N-isopropylamino)-diazen-1-ium-1,2-diolate
MbO_2	oxymyoglobin
MbNO	nitrosyl myoglobin
metMb	ferric myoglobin
mRNA	messenger RNA
NO	nitric oxide
NONOate	diazeniumdiolate

NONO-aspirin	adducts of aspirin with diazeniumdiolates
NSAID	non-steroidal anti-inflammatory drugs
PBS	phosphate-buffered saline
PGE_2	prostaglandin E_2
Piloty's salt	*N*-hydroxy-benzenesulfonamide
RPMI	Roswell Park Memorial Institute
RT-PCR	real-time polymerase chain reaction
TLC	thin layer chromatography

References

1. Wallace JL. Prostaglandins, NSAIDs, and gastric mucosal protection: Why doesn't the stomach digest itself? Physiol. Rev. 2008; 88:1547–1565. [PubMed: 18923189]
2. Luscher TF, Boulanger CM, Dohi Y, Yang ZH. Endothelium-derived contracting factors. Hypertension. 1992; 19:117–130. [PubMed: 1737645]
3. Davidge ST. Prostaglandin H synthase and vascular function. Circ. Res. 2001; 89:650–660. [PubMed: 11597987]
4. Cheng Y, Austin SC, Rocca B, Koller BH, Coffman TM, Grosser T, Lawson JA, FitzGerald GA. Role of Prostacyclin in the cardiovascular response to thromboxane A(2). Science. 2002; 296:539–541. [PubMed: 11964481]
5. Breyer MD, Breyer RM. Prostaglandin-E receptors and the kidney. Am. J. Physiol. Renal Physiol. 2000; 279:F12–F23. [PubMed: 10894784]
6. Cao CY, Matsumura K, Yamagata K, Watanabe Y. Involvement of cyclooxygenase-2 in LPS-induced fever and regulation of its mRNA by LPS in the rat brain. Am. J. Physiol.-Regul. Integr. Comp. Physiol. 1997; 272:R1712–R1725.
7. Kiyoshi M, Chunyu CAO, Yasuyoshi W. Possible role of cyclooxygenase-2 in the brain vasculature in febrile response. Ann. NY Acad. Sci. 1997; 813:302–306. [PubMed: 9100897]
8. Kawaguchi H, Pilbeam CC, Harrison JR, Raisz LG. The role of prostaglandins in the regulation of bone metabolism. Clin. Orthop. Rel. Res. 1995; 313:36–46.
9. Dubois RN, Abramson SB, Crofford L, Gupta RA, Simon LS, Van De Putte LB, Lipsky PE. Cyclooxygenase in biology and disease. FASEB J. 1998; 12:1063–1067. [PubMed: 9737710]
10. Cimino PJ, Keene CD, Breyer RM, Montine KS, Montine TJ. Therapeutic targets in prostaglandin E2 signaling for neurologic disease. Curr. Med. Chem. 2008; 15:1863–1869. [PubMed: 18691044]
11. Hein AM, O'Banion MK. Neuroinflammation and memory: the role of prostaglandins. Mol. Neurobiol. 2009; 40:15–32. [PubMed: 19365736]
12. Minghetti L. Cyclooxygenase-2 (COX-2) in inflammatory and degenerative brain diseases. J. Neuropathol. Exp. Neurol. 2004; 63:901–910. [PubMed: 15453089]
13. Kamei D, Murakami M, Nakatani Y, Ishikawa Y, Ishii T, Kudo I. Potential role of microsomal postaglandin E synthase-1 in tumorigenesis. J. Biol. Chem. 2003; 278:19396–19405. [PubMed: 12626523]
14. Vane JR. Inhibition of prostaglandin synthesis as a mechanism of action for aspirin-like drugs. Nature New Biol. 1971; 231:232–235. [PubMed: 5284360]
15. Wallace JL. Nonsteroidal anti-inflammatory drugs and gastroenteropathy: The second hundred years. Gastroenterology. 1997; 112:1000–1016. [PubMed: 9041264]
16. Seibert K, Zhang Y, Leahy K, Hauser S, Masferrer J, Perkins W, Lee L, Isakson P. Pharmacological and biochemical demonstration of the role of cyclooxygenase 2 in inflammation and pain. Proc. Natl. Acad. Sci. U.S.A. 1994; 91:12013–12017. [PubMed: 7991575]

17. Mitchell JA, Warner TD. COX isoforms in the cardiovascular system: understanding the activities of non-steroidal anti-inflammatory drugs. Nat Rev. Drug. Discov. 2006; 5:75–78. [PubMed: 16485347]
18. Everts B, Währborg P, Hedner T. COX-2-specific inhibitors - the emergence of a new class of analgesic and anti-inflammatory drugs. Clin. Rheumatol. 2000; 19:331–343. [PubMed: 11055820]
19. Antman EM, Bennett JS, Daugherty A, Furberg C, Roberts H, Taubert KA. Use of nonsteroidal antiinflammatory drugs: an update for clinicians: a scientific statement from the American Heart Association. Circulation. 2007; 115:1634–1642. [PubMed: 17325246]
20. Keeble JE, Moore PK. Pharmacology and potential therapeutic applications of nitric oxide-releasing non-steroidal anti-inflammatory and related nitric oxide-donating drugs. Br. J. Pharmacol. 2002; 137:295–310. [PubMed: 12237248]
21. Flaherty JT, Reid PR, Kelly DT, Taylor DR, Weisfeldt ML, Pitt B. Intravenous nitroglycerin in acute myocardial-infarction. Circulation. 1975; 51:132–139. [PubMed: 803231]
22. Rigas B, Kashfi K. Nitric-oxide-donating NSAIDs as agents for cancer prevention. Trends Mol. Med. 2004; 10:324–330. [PubMed: 15242680]
23. Minamiyama Y, Takemura S, Nishino Y, Okada S. Organic nitrate tolerance is induced by degradation of some cytochrome P450 isoforms. Redox Rep. 2002; 7:339–342. [PubMed: 12688525]
24. Thatcher GRJ. NO problem for nitroglycerin: organic nitrate chemistry and therapy. Chem. Soc. Rev. 1998; 27:331–337.
25. Torfgård KE, Ahlner J. Mechanisms of action of nitrates. Cardiovasc. Drugs Ther. 1994; 8:701–717. [PubMed: 7873467]
26. Hulsman N, Medema JP, Bos C, Jongejan A, Leurs R, Smit MJ, de Esch IJP, Richel D, Wijtmans M. Chemical insights in the concept of hybrid drugs: The antitumor effect of nitric oxide-donating aspirin involves a quinone methide but not nitric oxide nor aspirin. J. Med. Chem. 2007; 50:2424–2431. [PubMed: 17441704]
27. Velázquez C, Rao PNP, Knaus EE. Novel nonsteroidal antiinflammatory drugs possessing a nitric oxide donor diazen-1-ium-1,2-diolate moiety: Design, synthesis, biological evaluation, and nitric oxide release studies. J. Med. Chem. 2005; 48:4061–4067. [PubMed: 15943479]
28. Velázquez CA, Rao PNP, Citro ML, Keefer LK, Knaus EE. O^2-Acetoxymethyl-protected diazeniumdiolate-based NSAIDs (NONO-NSAIDs): synthesis, nitric oxide release, and biological evaluation studies. Bioorg. Med. Chem. 2007; 15:4767–4774. [PubMed: 17509888]
29. Maragos CM, Morley D, Wink DA, Dunams TM, Saavedra JE, Hoffman A, Bove AA, Isaac L, Hrabie JA, Keefer LK. Complexes of NO with nucleophiles as agents for the controlled biological release of nitric oxide - vasorelaxant effects. J. Med. Chem. 1991; 34:3242–3247. [PubMed: 1956043]
30. Keefer LK. Nitric oxide (NO)- and nitroxyl (HNO)-generating diazeniumdiolates (NONOates): Emerging commercial opportunities. Curr. Top. Med. Chem. 2005; 5:625–634. [PubMed: 16101424]
31. Dutton AS, Fukuto JM, Houk KN. Mechanisms of HNO and NO production from Angeli's salt: Density functional and CBS-QB3 theory predictions. J. Am. Chem. Soc. 2004; 126:3795–3800. [PubMed: 15038733]
32. Dutton AS, Suhrada CP, Miranda KM, Wink DA, Fukuto JM, Houk KN. Mechanism of pH-dependent decomposition of monoalkylamine diazeniumdiolates to form HNO and NO, deduced from the model compound methylamine diazeniumdiolate, density functional theory, and CBS-QB3 calculations. Inorg. Chem. 2006; 45:2448–2456. [PubMed: 16529464]
33. Salmon DJ, Torres de Holding CL, Thomas L, Peterson KV, Goodman GP, Saavedra JE, Srinivasan A, Davies KM, Keefer LK, Miranda KM. HNO and NO release from a arimary amine-based diazeniumdiolate as a function of pH. Inorg. Chem. 2011; 50:3262–3270. [PubMed: 21405089]
34. Paolocci N, Katori T, Champion HC, St. John ME, Miranda KM, Fukuto JM, Wink DA, Kass DA. Positive inotropic and lusitropic effects of HNO/NO- in failing hearts: independence from b-adrenergic signaling. Proc. Natl. Acad. Sci. U.S.A. 2003; 100:5537–5542. [PubMed: 12704230]

35. Paolocci N, Saavedra WF, Miranda KM, Martignani C, Isoda T, Hare JM, Espey MG, Fukuto JM, Feelisch M, Wink DA, Kass DA. Nitroxyl anion exerts redox-sensitive positive cardiac inotropy in vivo by calcitonin gene-related peptide signaling. Proc. Natl. Acad. Sci. U. S. A. 2001; 98:10463–10468. [PubMed: 11517312]
36. Norris AJ, Sartippour MR, Lu M, Park T, Rao JY, Jackson MI, Fukuto JM, Brooks MN. Nitroxyl inhibits breast tumor growth and angiogenesis. Int. J. Cancer. 2008; 122:1905–1910. [PubMed: 18076071]
37. Nagasawa HT, Kawle SP, Elberling JA, Demaster EG, Fukuto JM. Prodrugs of nitroxyl as potential aldehyde dehydrogenase inhibitors vis-a-vis vascular smooth-muscle relaxants. J. Med. Chem. 1995; 38:1865–1871. [PubMed: 7783118]
38. Saavedra JE, Bohle DS, Smith KN, George C, Deschamps JR, Parrish D, Ivanic J, Wang YN, Citro ML, Keefer LK. Chemistry of the diazeniumdiolates. O- versus N-alkylation of the RNH[N(O)NO](-) ion. J. Am. Chem. Soc. 2004; 126:12880–12887. [PubMed: 15469285]
39. Andrei D, Salmon DJ, Donzelli S, Wahab A, Klose JR, Citro ML, Saavedra JE, Wink DA, Miranda KM, Keefer LK. Dual mechanisms of HNO generation by a nitroxyl prodrug of the diazeniumdiolate (NONOate) class. J. Am. Chem. Soc. 2010; 132:16526–16532. [PubMed: 21033665]
40. Saavedra JE, Shami PJ, Wang LY, Davies KM, Booth MN, Citro ML, Keefer LK. Esterase-sensitive nitric oxide donors of the diazeniumdiolate family: In vitro antileukemic activity. J. Med. Chem. 2000; 43:261–269. [PubMed: 10649981]
41. Tang X, Xian M, Trikha M, Honn KV, Wang PG. Synthesis of peptide-diazeniumdiolate conjugates: towards enzyme activated antitumor agents. Tetrahedron Lett. 2001; 42:2625–2629.
42. Shafirovich V, Lymar SV. Nitroxyl and its anion in aqueous solutions: Spin states, protic equilibria, and reactivities toward oxygen and nitric oxide. Proc. Natl. Acad. Sci. U. S. A. 2002; 99:7340–7345. [PubMed: 12032284]
43. Miranda KM, Katori T, Torres de Holding CL, Thomas L, Ridnour LA, McLendon WJ, Cologna SM, Dutton AS, Champion HC, Mancardi D, Tocchetti CG, Saavedra JE, Keefer LK, Houk KN, Fukuto JM, Kass DA, Paolocci N, Wink DA. Comparison of the NO and HNO donating properties of diazeniumdiolates: primary amine adducts release HNO in vivo. J. Med. Chem. 2005; 48:8220–8228. [PubMed: 16366603]
44. Andersen HJ, Skibsted LH. Kinetics and mechanism of thermal-oxidation and photooxidation of nitrosylmyoglobin in aqueous solution. J. Agric. Food Chem. 1992; 40:1741–1750.
45. Doyle MP, Pickering RA, Cook BR. Oxidation of oxymyoglobin by nitric oxide through dissociation from cobalt nitrosyls. J. Inorg. Biochem. 1983; 19:329–338.
46. Doyle MP, Hoekstra JW. Oxidation of nitrogen oxides by bound dioxygen in hemoproteins. J. Inorg. Biochem. 1981; 14:351–358. [PubMed: 7276933]
47. Miranda KM, Paolocci N, Katori T, Thomas DD, Ford E, Bartberger MD, Espey MG, Kass DA, Feelisch M, Fukuto JM, Wink DA. A biochemical rationale for the discrete behavior of nitroxyl and nitric oxide in the cardiovascular system. Proc. Natl. Acad. Sci. U.S.A. 2003; 100:9196–9201. [PubMed: 12865500]
48. Pryor WA, Church DF, Govindan CK, Crank G. Oxidation of thiols by nitric oxide and nitrogen dioxide - synthetic utility and toxicological implications. J. Org. Chem. 1982; 47:156–159.
49. Tang J, Faustman C, Lee S, Hoagland TA. Effect of glutathione on oxymyoglobin oxidation. J. Agric. Food Chem. 2003; 51:1691–1695. [PubMed: 12617606]
50. Wink DA, Feelisch M, Fukuto J, Chistodoulou D, Jourd'heuil D, Grisham MB, Vodovotz Y, Cook JA, Krishna M, DeGraff WG, Kim S, Gamson J, Mitchell JB. The cytotoxicity of nitroxyl: Possible implications for the pathophysiological role of NO. Arch. Biochem. Biophys. 1998; 351:66–74. [PubMed: 9501920]
51. Kojima H, Sakurai K, Kikuchi K, Kawahara S, Kirino Y, Nagoshi H, Hirata Y, Nagano T. Development of a fluorescent indicator for nitric oxide based on the fluorescein chromophore. Chem. Pharm. Bull. 1998; 46:373–375. [PubMed: 9501473]
52. Espey MG, Miranda KM, Thomas DD, Wink DA. Ingress and reactive chemistry of nitroxyl-derived species within human cells. Free Radic. Biol. Med. 2002; 33:827–834. [PubMed: 12208370]

53. Davies NM, Sharkey KA, Asfaha S, Macnaughton WK, Wallace JL. Aspirin causes rapid up-regulation of cyclo-oxygenase-2 expression in the stomach of rat. Aliment. Pharmacol. Ther. 1997; 11:1101–1108. [PubMed: 9663836]
54. Huang M, Stolina M, Sharma S, Mao JT, Zhu L, Miller PW, Wollman J, Herschman H, Dubinett SM. Non-small cell lung cancer cyclooxygenase-2-dependent regulation of cytokine balance in lymphocytes and macrophages: Up-regulation of interleukin 10 and down-regulation of interleukin 12 production. Cancer Res. 1998; 58:1208–1216. [PubMed: 9515807]
55. Williams CS, Smalley W, DuBois RN. Aspirin use and potential mechanisms for colorectal cancer preventionn. J. Clin. Invest. 1997; 100:1325–1329. [PubMed: 9294096]
56. Rouzer CA, Marnett LJ. Cyclooxygenases: structural and functional insights. J. Lipid Res. 2009; 50:S29–S34. [PubMed: 18952571]
57. Kennedy TA, Smith CJ, Marnett LJ. Investigation of the role of cysteines in catalysis by prostaglandin endoperoxide synthase. J. Biol. Chem. 1994; 269:27357–27364. [PubMed: 7961646]
58. Lopez BE, Rodriguez CE, Pribadi M, Cook NM, Shinyashiki M, Fukuto JM. Inhibition of yeast glycolysis by nitroxyl (HNO): A mechanism of HNO toxicity and implications to HNO biology. Arch. Biochem. Biophys. 2005; 442:140–148. [PubMed: 16139238]
59. Lopez BE, Wink DA, Fukuto JM. The inhibition of glyceraldehyde-3-phosphate dehydrogenase by nitroxyl (HNO). Arch. Biochem. Biophys. 2007; 465:430–436. [PubMed: 17678614]
60. Shen B, English AM. Mass spectrometric analysis of nitroxyl-mediated protein modification: Comparison of products formed with free and protein-based cysteines. Biochemistry. 2005; 44:14030–14044. [PubMed: 16229492]
61. Schreinemachers DM, Everson RB. Aspirin use and lung, colon, and breast cancer incidence in a prospective study. Epidemiology. 1994; 5:138–146. [PubMed: 8172988]
62. Harris RE, Beebe-Donk J, Doss H, Doss DB. Aspirin, ibuprofen, and other non-steroidal anti-inflammatory drugs in cancer prevention: A critical review of non-selective COX-2 blockade (review). Oncol. Rep. 2005; 13:559–583. [PubMed: 15756426]
63. Fosslien E. Molecular pathology of cyclooxygenase-2 in neoplasia. Ann. Clin. Lab. Sci. 2000; 30:3–21. [PubMed: 10678579]
64. Howe LR, Subbaramaiah K, Brown AM, Dannenberg AJ. Cyclooxygenase-2: a target for the prevention and treatment of breast cancer. Endocr. Relat. Cancer. 2001; 8:97–114. [PubMed: 11397667]
65. Pai R, Nakamura T, Moon WS, Tarnawski AS. Prostaglandins promote colon cancer cell invasion; signaling by cross-talk between two distinct growth factor receptors. FASEB J. 2003; 17:1640–1647. [PubMed: 12958170]
66. Fulton AM, Zhang SZ, Chong YC. Role of the prostaglandin E2 receptor in mammary tumor metastasis. Cancer Res. 1991; 51:2047–2050. [PubMed: 1849040]
67. Wang D, DuBois RN. The role of COX-2 in intestinal inflammation and colorectal cancer. Oncogene. 2009; 29:781–788. [PubMed: 19946329]
68. Trifan OC, Hla TJ. Cyclooxygenase-2 modulates cellular growth and promotes tumorigenesis. Cell. Mol. Biol. 2003; 7:207–222.
69. Leahy KM, Koki AT, Masferrer JL. Role of cyclooxygenases in angiogenesis. Curr. Med. Chem. 2000; 7:1163–1170. [PubMed: 11032965]
70. Ruegg C, Dormond O, Mariotti A. Endothelial cell integrins and COX-2: mediators and therapeutic targets of tumor angiogenesis. Biochim. Biophys. Acta-Rev. Cancer. 2004; 1654:51–67.
71. Gately S. The contributions of cyclooxygenase-2 to tumor angiogenesis. Cancer Metastasis Rev. 2000; 19:19–27. [PubMed: 11191059]
72. Harris SG, Padilla J, Koumas L, Ray D, Phipps RP. Prostaglandins as modulators of immunity. Trends Immunol. 2002; 23:144–150. [PubMed: 11864843]
73. Wilson KT, Fu S, Ramanujam KS, Meltzer SJ. Increased expression of inducible nitric oxide synthase and cyclooxygenase-2 in Barrett's esophagus and associated adenocarcinomas. Cancer Res. 1998; 58:2929–2934. [PubMed: 9679948]

74. Chiarugi V, Magnelli L, Gallo O. Cox-2, iNOS and p53 as play-makers of tumor angiogenesis. Int. J. Mol. Med. 1998; 2:715–719. [PubMed: 9850741]
75. Mocellin S, Bronte V, Nitti D. Nitric oxide, a double edged sword in cancer biology: Searching for therapeutic opportunities. Med. Res. Rev. 2007; 27:317–352. [PubMed: 16991100]
76. Stoyanovsky DA, Schor NF, Nylander KD, Salama G. Effects of pH on the cytotoxicity of sodium trioxodinitrate (Angeli's salt). J. Med. Chem. 2004; 47:210–217. [PubMed: 14695834]
77. Nath N, Vassell R, Chattopadhyay M, Kogan M, Kashfi K. Nitro-aspirin inhibits MCF-7 breast cancer cell growth: effects on COX-2 expression and Wnt/beta-catenin/TCF-4 signaling. Biochem. Pharmacol. 2009; 78:1298–1304. [PubMed: 19576865]
78. Hockel M, Vaupel P. Tumor hypoxia: Definitions and current clinical, biologic, and molecular aspects. J. Natl. Cancer Inst. 2001; 93:266–276. [PubMed: 11181773]
79. Gatenby RA, Gillies RJ. Why do cancers have high aerobic glycolysis? Nat. Rev. Cancer. 2007; 4:891–899. [PubMed: 15516961]
80. Gatenby RA, Gillies RJ. Glycolysis in cancer: a potential target for therapy. Int. J. Biochem. Cell Biol. 2007; 39:1358–1366. [PubMed: 17499003]
81. Sirover MA. New nuclear functions of the glycolytic protein, glyceraldehyde-3-phosphate dehydrogenase, in mammalian cells. J. Cell. Biochem. 2005; 95:45–52. [PubMed: 15770658]
82. Colell A, Green DR, Ricci JE. Novel roles for GAPDH in cell death and carcinogenesis. Cell Death Differ. 2009; 16:1573–1581. [PubMed: 19779498]
83. Catella-Lawson F, Reilly MP, Kapoor SC, Cucchiara AJ, DeMarco S, Tournier B, Vyas SN, FitzGerald GA. Cyclooxygenase inhibitors and the antiplatelet effects of aspirin. N. Engl. J. Med. 2001; 345:1809–1817. [PubMed: 11752357]
84. Fosbol EL, Folke F, Jacobsen S, Rasmussen JN, Sorensen R, Schramm TK, Andersen SS, Rasmussen S, Poulsen HE, Kober L, Torp-Pedersen C, Gislason GH. Cause-specific cardiovascular risk associated with nonsteroidal antiinflammatory drugs among healthy individuals. Circ. Cardiovasc. Qual. Outcomes. 2010; 3:395–403. [PubMed: 20530789]
85. Ma XL, Gao F, Liu GL, Lopez BL, Christopher TA, Fukuto JM, Wink DA, Feelisch M. Opposite effects of nitric oxide and nitroxyl on postischemic myocardial injury. Proc. Natl. Acad. Sci. U.S.A. 1999; 96:14617–14622. [PubMed: 10588754]
86. Tocchetti CG, Wang W, Froehlich JP, Huke S, Aon MA, Wilson GM, Di Benedetto G, O'Rourke B, Gao WD, Wink DA, Toscano JP, Zaccolo M, Bers DM, Valdivia HH, Cheng H, Kass DA, Paolocci N. Nitroxyl improves cellular heart function by directly enhancing cardiac sarcoplasmic reticulum Ca^{2+} cycling. Circ. Res. 2007; 100:96–104. [PubMed: 17138943]
87. Froehlich JP, Mahaney JE, Keceli G, Pavlos CM, Goldstein R, Redwood AJ, Sumbilla C, Lee DI, Tocchetti CG, Kass DA, Paolocci N, Toscano JP. Phospholamban thiols play a central role in activation of the cardiac muscle sarcoplasmic reticulum calcium pump by nitroxyl. Biochemistry. 2008; 47:13150–13152. [PubMed: 19053265]
88. Kohr MJ, Kaludercic N, Tocchetti CG, Dong Gao W, Kass DA, Janssen PM, Paolocci N, Ziolo MT. Nitroxyl enhances myocyte Ca^{2+} transients by exclusively targeting SR Ca2+-cycling. Front. Biosci. 2010; 2:614–626.
89. Drago RS, Karstetter BR. The reaction of nitrogen(II) oxide with various primary and secondary amines. J. Am. Chem. Soc. 1961; 83:1819–1822.
90. Lopez BE, Shinyashiki M, Han TH, Fukuto JM. Antioxidant actions of nitroxyl (HNO). Free Radic. Biol. Med. 2007; 42:482–491. [PubMed: 17275680]
91. Miranda KM, Nagasawa HT, Toscano JP. Donors of HNO. Curr. Top. Med. Chem. 2005; 5:649–664. [PubMed: 16101426]
92. Doyle MP, Mahapatro SN. Nitric-Oxide Dissociation from trioxodinitrate(II) in aqueous solution. J. Am. Chem. Soc. 1984; 106:3678–3679.
93. Kojima H, Nakatsubo N, Kikuchi K, Kawahara S, Kirino Y, Nagoshi H, Hirata Y, Nagano T. Detection and imaging of nitric oxide with novel fluorescent indicators: Diaminofluoresceins. Anal. Chem. 1998; 70:2446–2453. [PubMed: 9666719]
94. Winter CAR, E. A. Nuss GW. Carrageenan-induced edema in hind paw of the rat as an assay for anti-inflammatory drugs. Proc. Soc. Exp. Biol. Med. 1962; 111:544–552. [PubMed: 14001233]

95. Cocco MT, Congiu C, Onnis V, Morelli M, Felipo V, Cauli O. Synthesis of new 2-arylamino-6-trifluoromethylpyridine-3-carboxylic acid derivatives and investigation of their analgesic activity. Bioorg. Med. Chem. 2004; 12:4169–4177. [PubMed: 15246093]

96. Bassani RA, Bassani JWM, Bers DM. Mitochondrial and sarcolemmal Ca^{2+} transport reduce $[Ca^{2+}]_i$ during caffeine contractures in rabbit cardiac myocytes. J. Physiol. 1992; 453:591–608. [PubMed: 1464847]

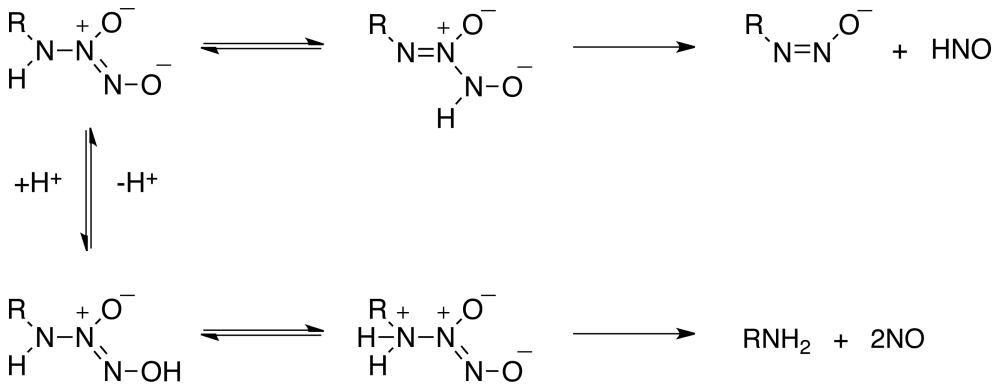

Scheme 1.
Dual decomposition mechanisms available for primary amine diazeniumdiolates leading to release of HNO or NO.

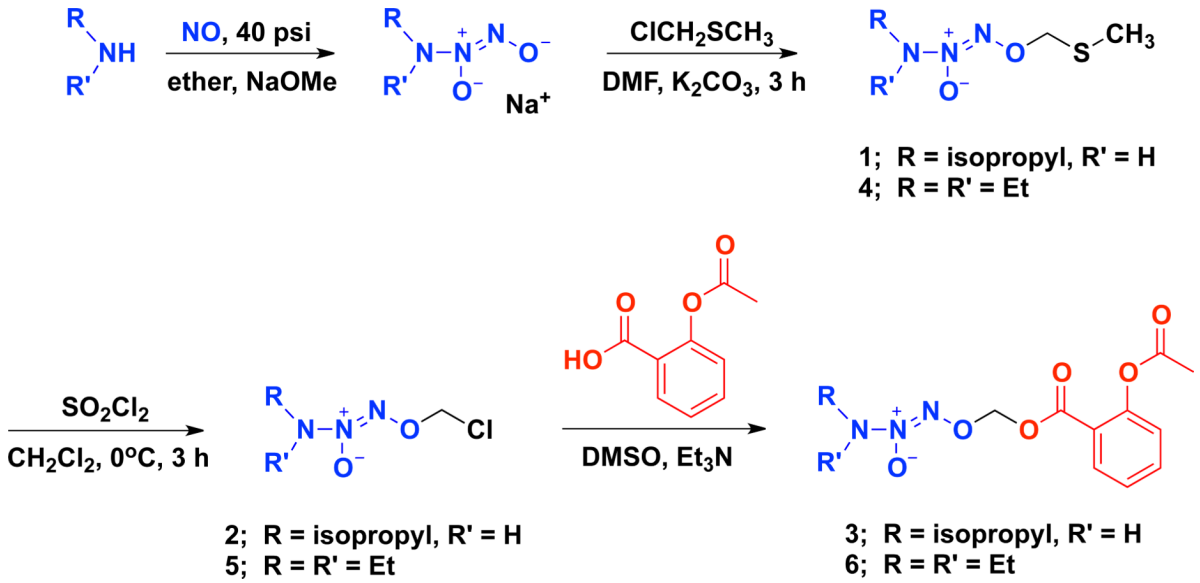

Scheme 2.
Synthesis of NO or HNO releasing aspirin prodrugs.

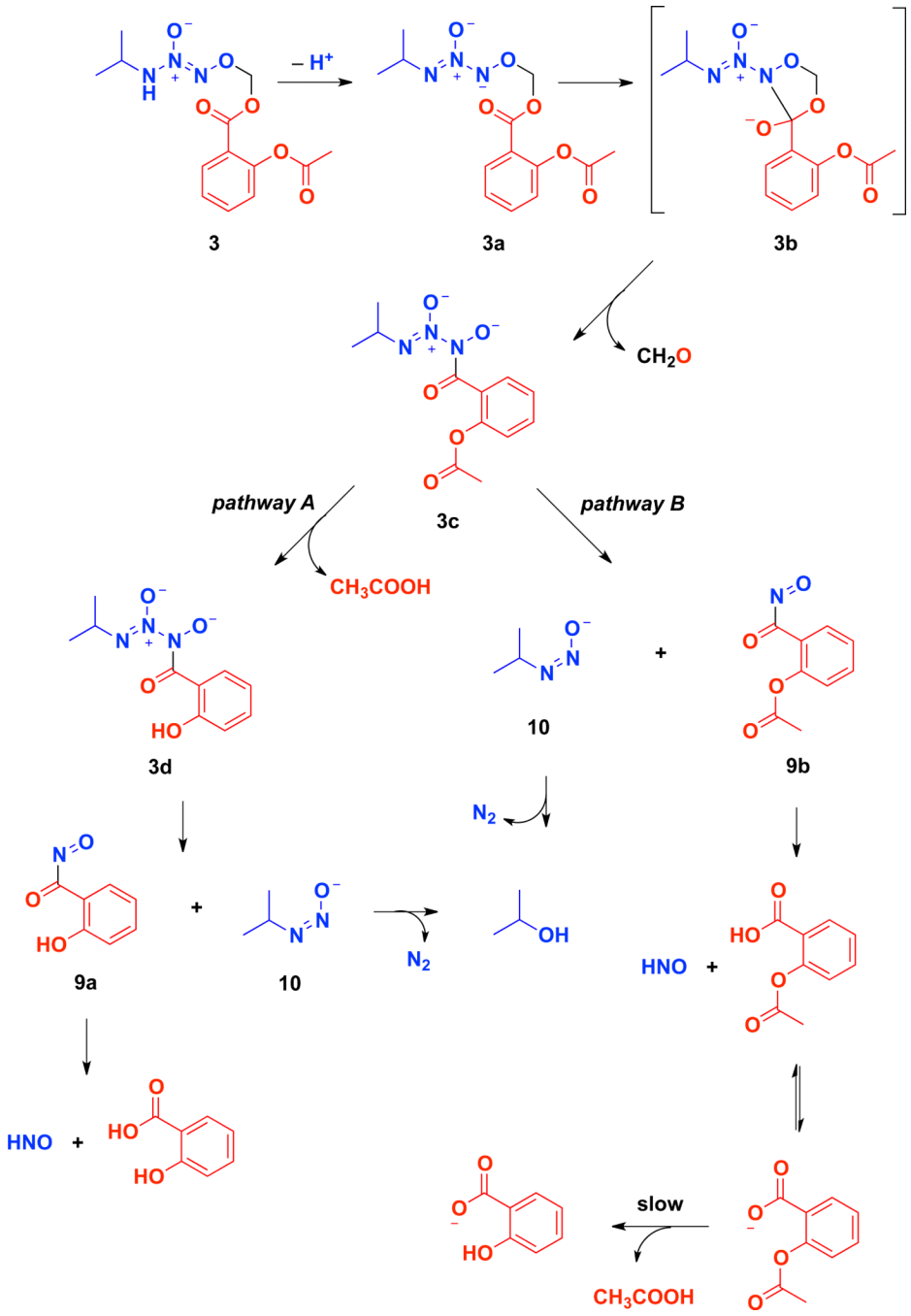

Scheme 3.
Possible pathways leading to HNO and salicylate production from spontaneous decomposition of IPA/NO-aspirin via initial amine deprotonation.

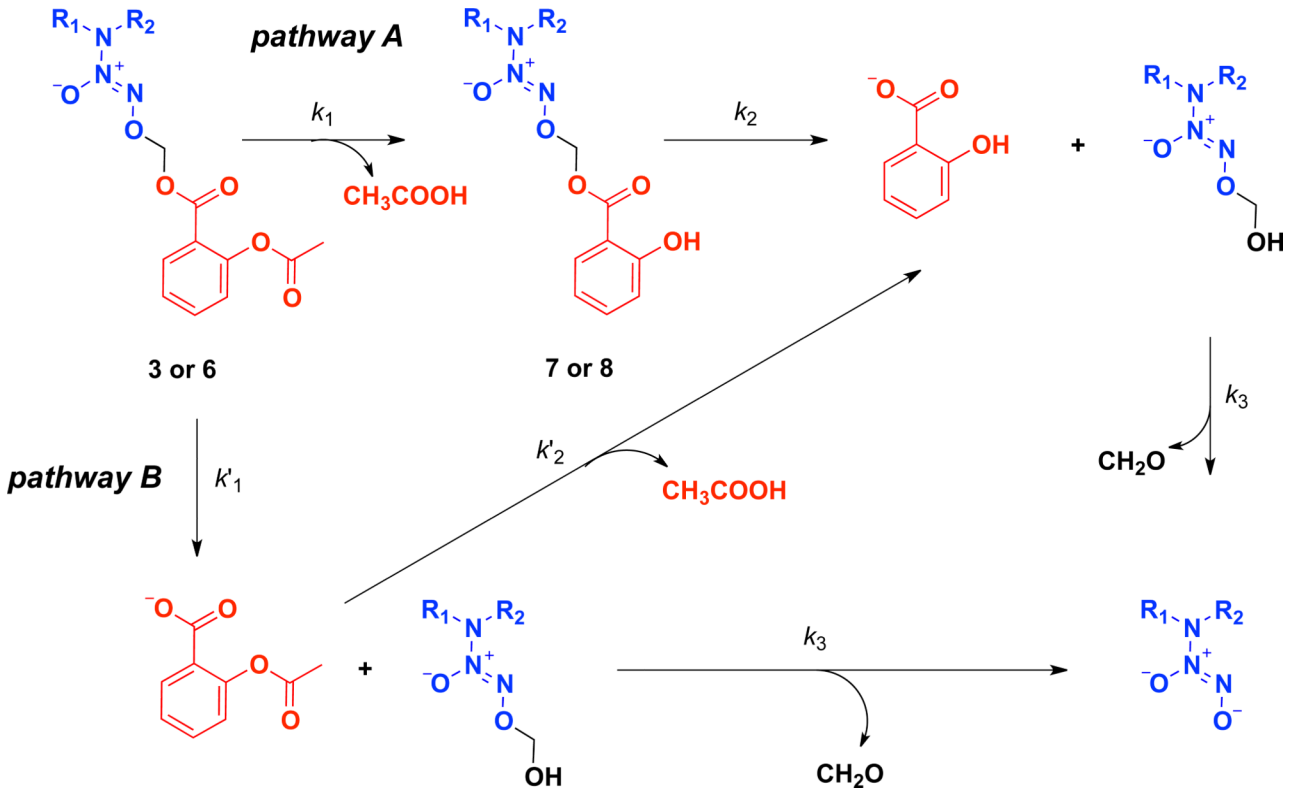

Scheme 4.

Possible pathways leading to salicylate and free diazeniumdiolate production from spontaneous decomposition of NONO-aspirin prodrugs via initial ester hydrolysis.

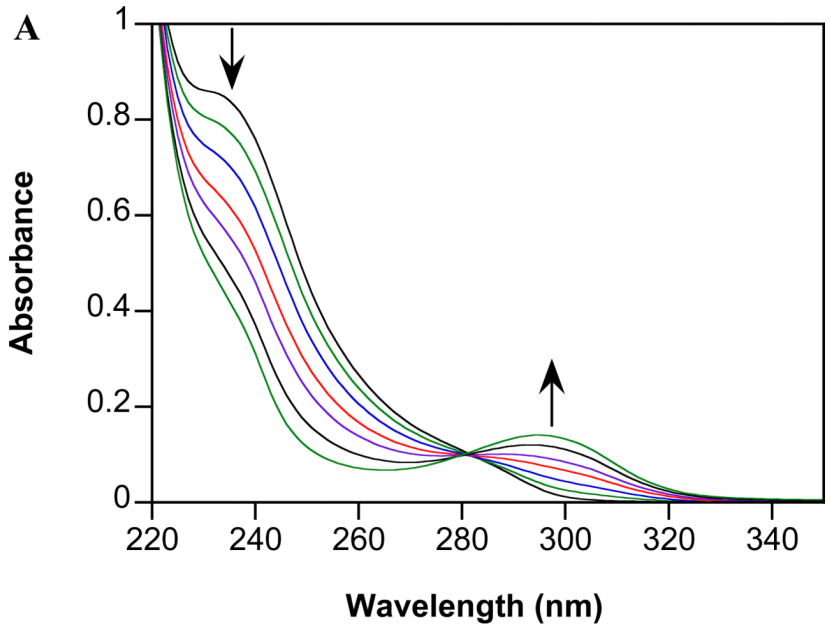

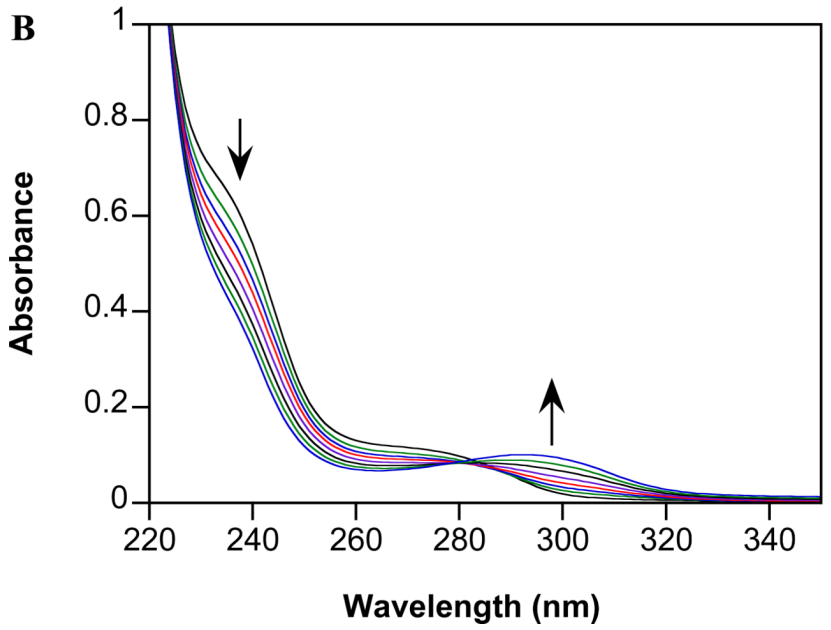

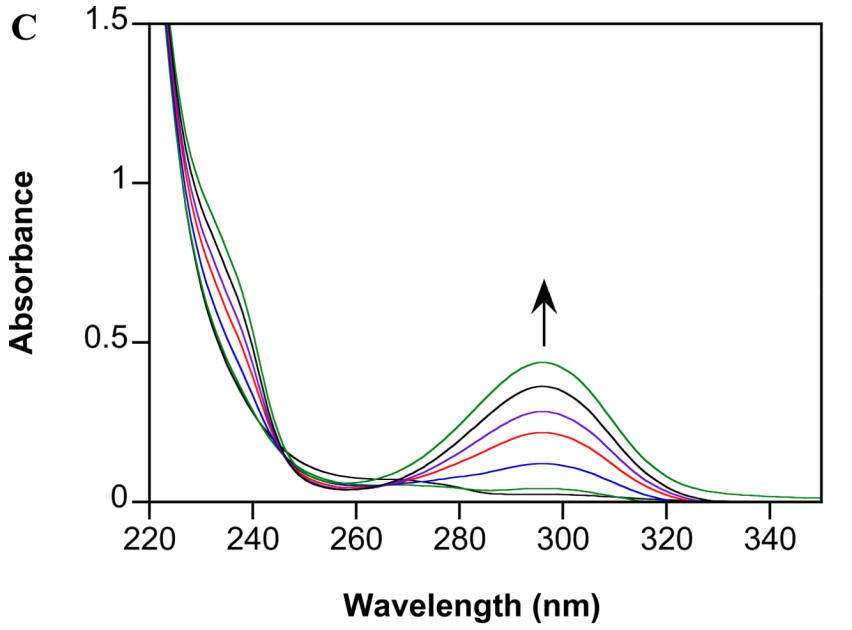

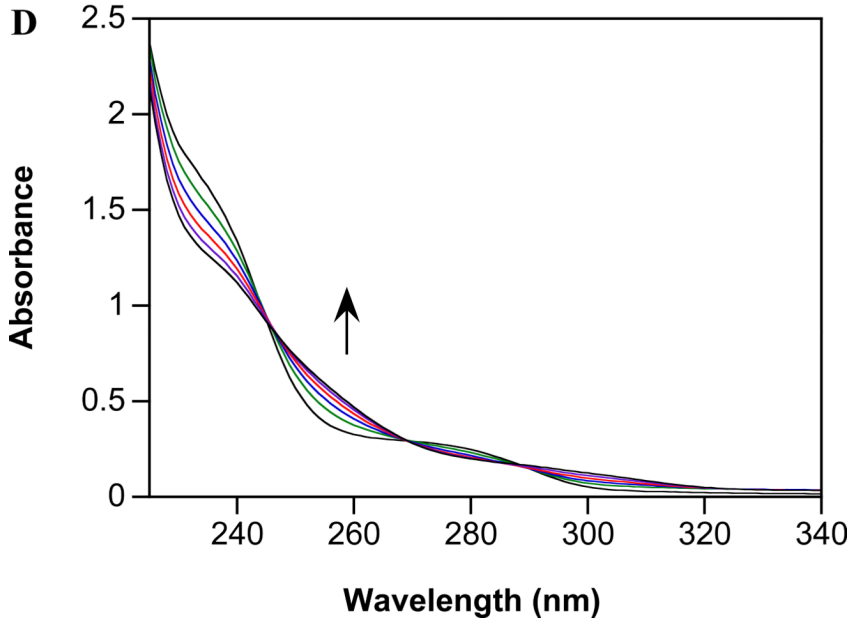

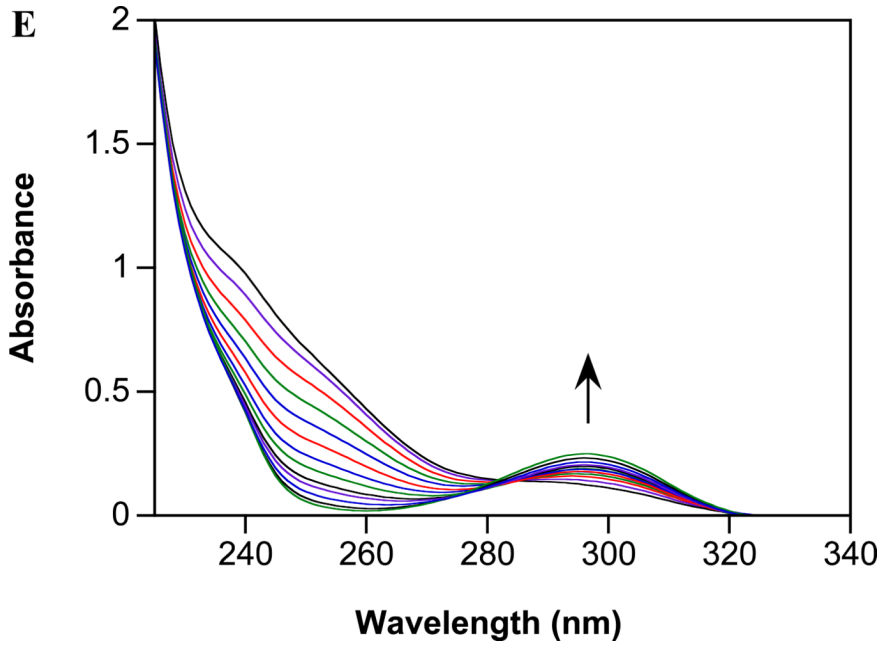

Figure 1.

Spontaneous hydrolysis of (**A**) IPA/NO-aspirin, (**B**) DEA/NO-aspirin or (**C**) aspirin at pH 7.4 and (**D, E**) DEA/NO-aspirin at pH 10 in PBS containing 50 μM DTPA at 37°C. Scans are plotted at 0, 90, 210, 390, 570, 930, 1410 min in (**A**), 60, 570, 930, 1290, 1770, 2370, 2970, 3690 min in (**B**), 60, 210, 570, 1170, 1770, 2970, 5730 min in (**C**), 0, 10, 20, 30, 40, 50 min in **(D)** and 80, 110, 150, 190, 230, 270, 320, 360, 420, 460, 540, 660, 820 min in **(E)**. The respective first-order rate constants of IPA/NO-aspirin and DEA/NO-aspirin decomposition at 241 nm are $(2.6 \pm 0.2) \times 10^{-5}$ s^{-1} ($n > 3$) and 5.3×10^{-6} s^{-1} ($n = 1$ given the slow rate) while that of aspirin at 295 nm is 9.8×10^{-6} s^{-1} ($n = 1$ given the slow rate); all $R^2 > 0.997$.

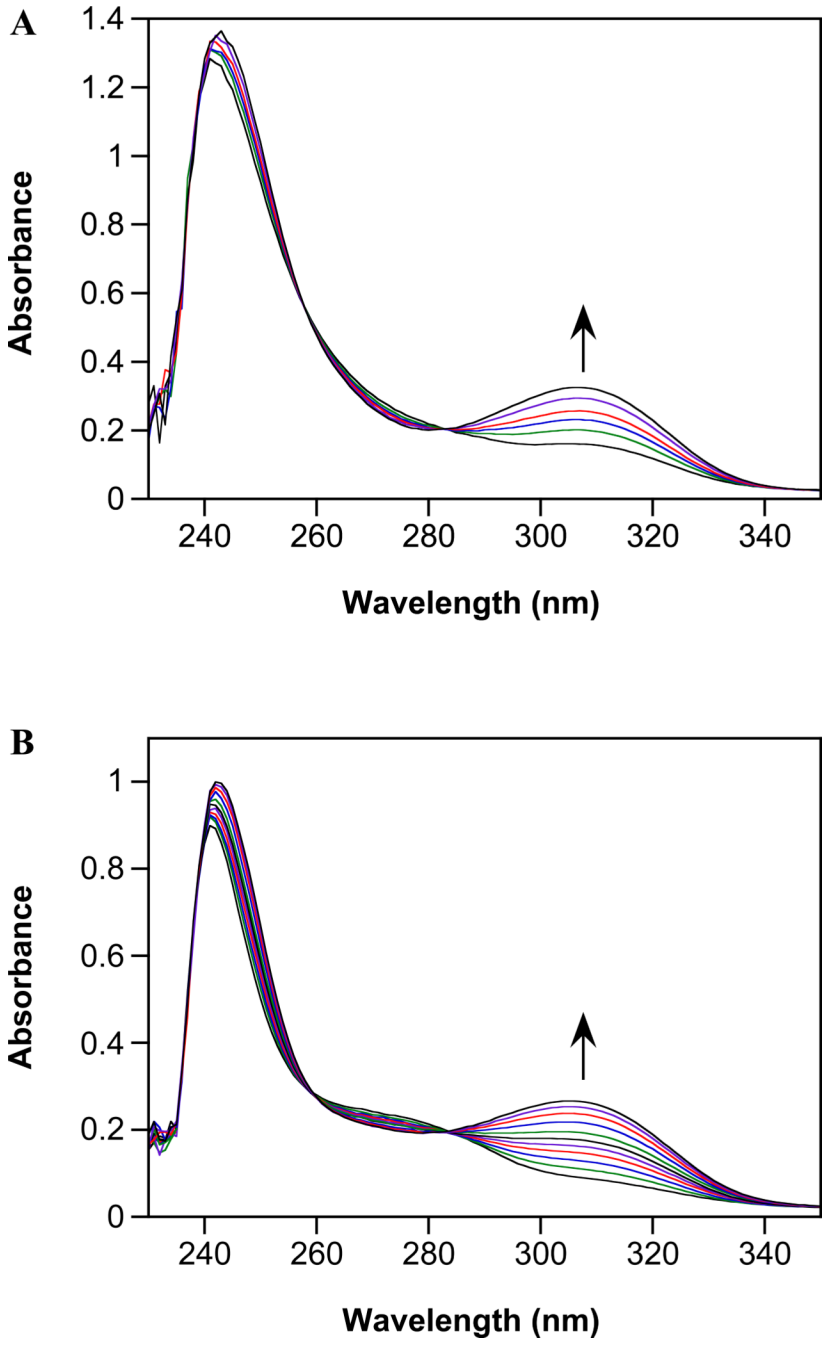

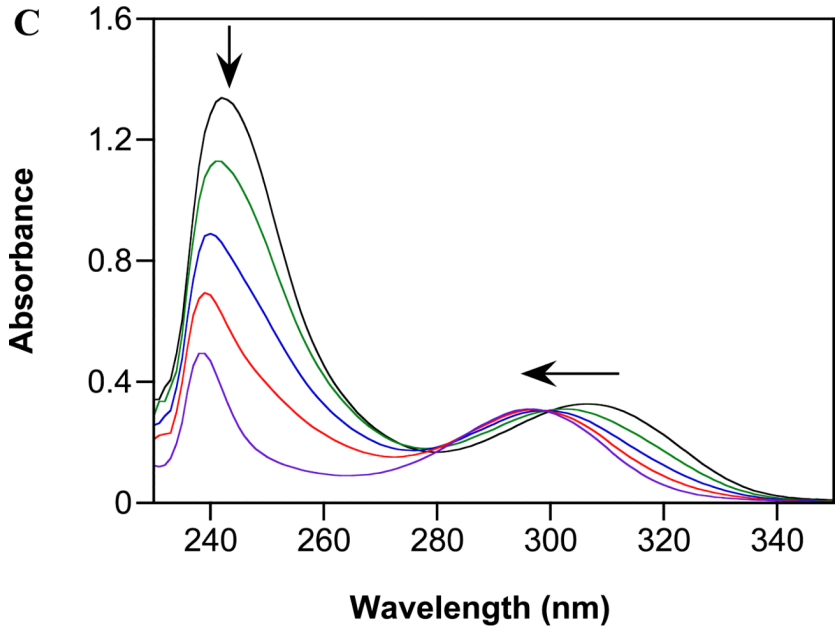

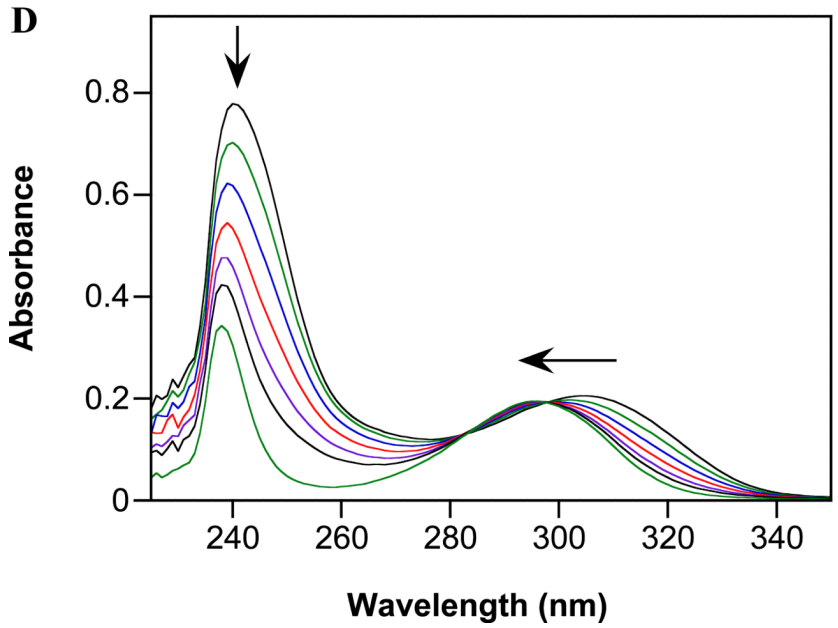

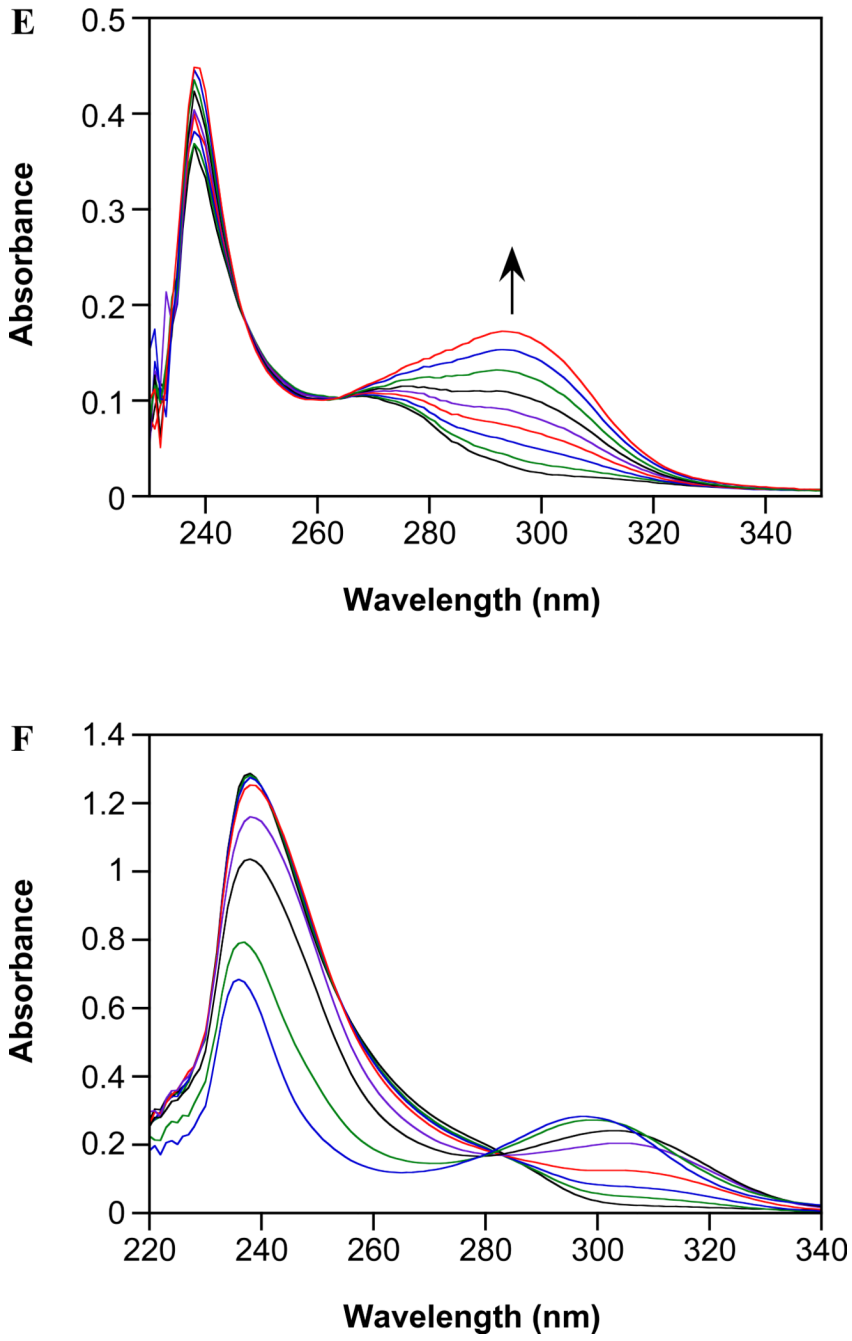

Figure 2.

Guinea pig serum induced hydrolysis of (**A**, **C**) IPA/NO-aspirin, (**B**, **D**) DEA/NO-aspirin, or (**E**) aspirin in PBS containing 50 μM DTPA at pH 7.4 and 37°C. Scans are plotted at 0, 5, 10, 15, 20, 25, 40 s in (**A**), 0, 5, 10, 15, 20, 25, 30, 40, 50, 60, 70 s in (**B**), 2, 14, 26, 38, 62 min in (**C**), 3, 6, 9, 12, 15, 18, 39 min in (**D**) and 1, 7, 19, 31, 43, 59, 79, 99, 119 min in (**E**). Panel (**F**) is as in (**A**) with the substitution of fetal bovine serum; scans are plotted at 0, 15, 30, 60, 150, 255, 555 and 885 min. All kinetic data fit to a first order equation ($n \geq 3$ except for $n = 1$ for **F**) with $R^2 > 0.983$. The presence of serum proteins impacts the blank-corrected spectra in the low 200 nm region in Figure 2 compared to Figure 1.

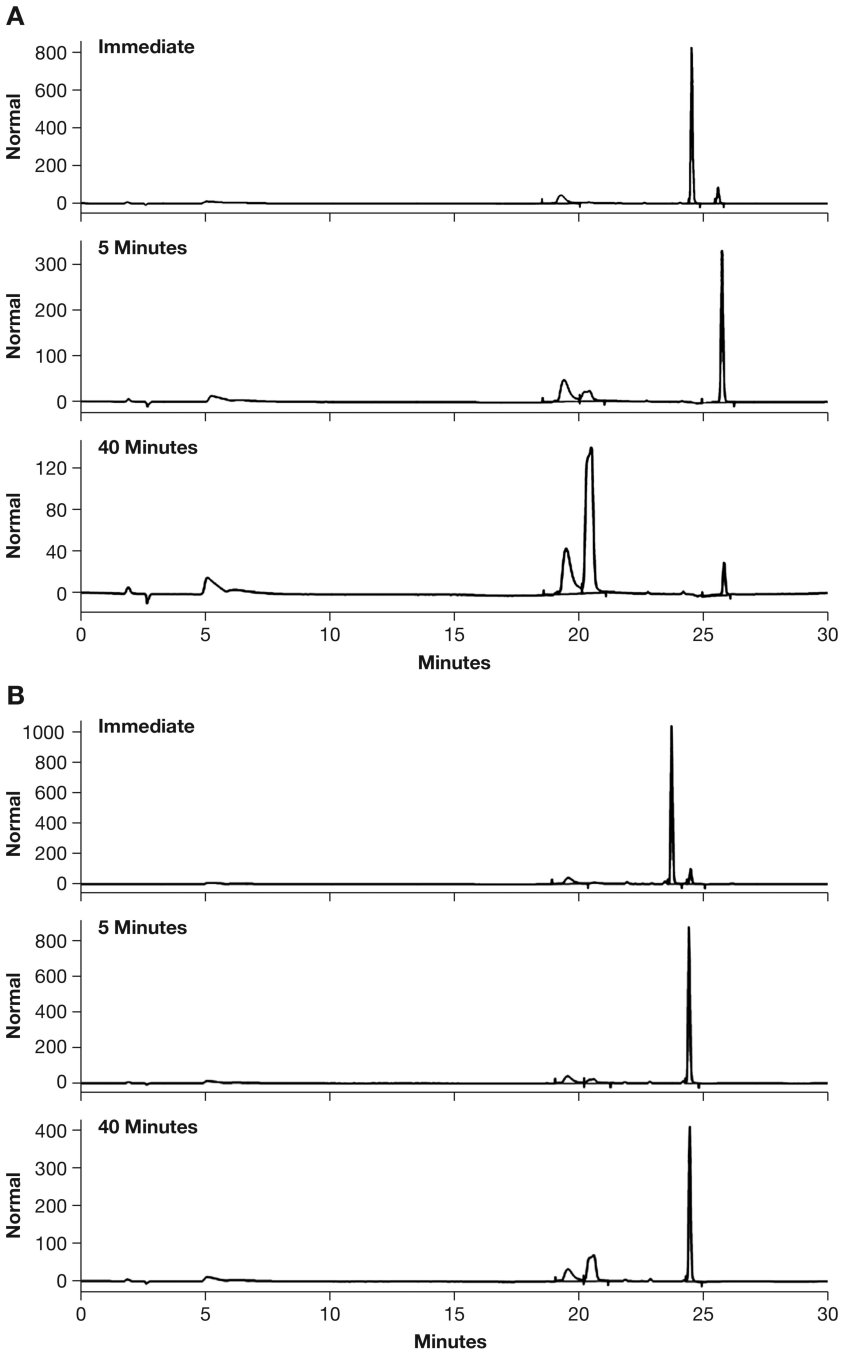

Figure 3.

HPLC analysis of guinea pig serum induced hydrolysis of (**A**) DEA/NO-aspirin or (**B**) IPA/NO-aspirin (100 μM) in 100 mM phosphate buffer containing 50 μM DTPA at pH 7.4 and 37°C. Authentic standards eluted from a Phenomenex Luna C18 column, 3 μm, 150 × 2.1 mm, using a water and acetonitrile gradient containing 0.1% formic acid as follows: aspirin (19.6 min), salicylate (20.5 min), IPA/NO-aspirin (23.8 min), IPA/NO-salicylate (24.6 min), DEA/NO-aspirin (24.6 min) and DEA/NO-salicylate (25.7 min).

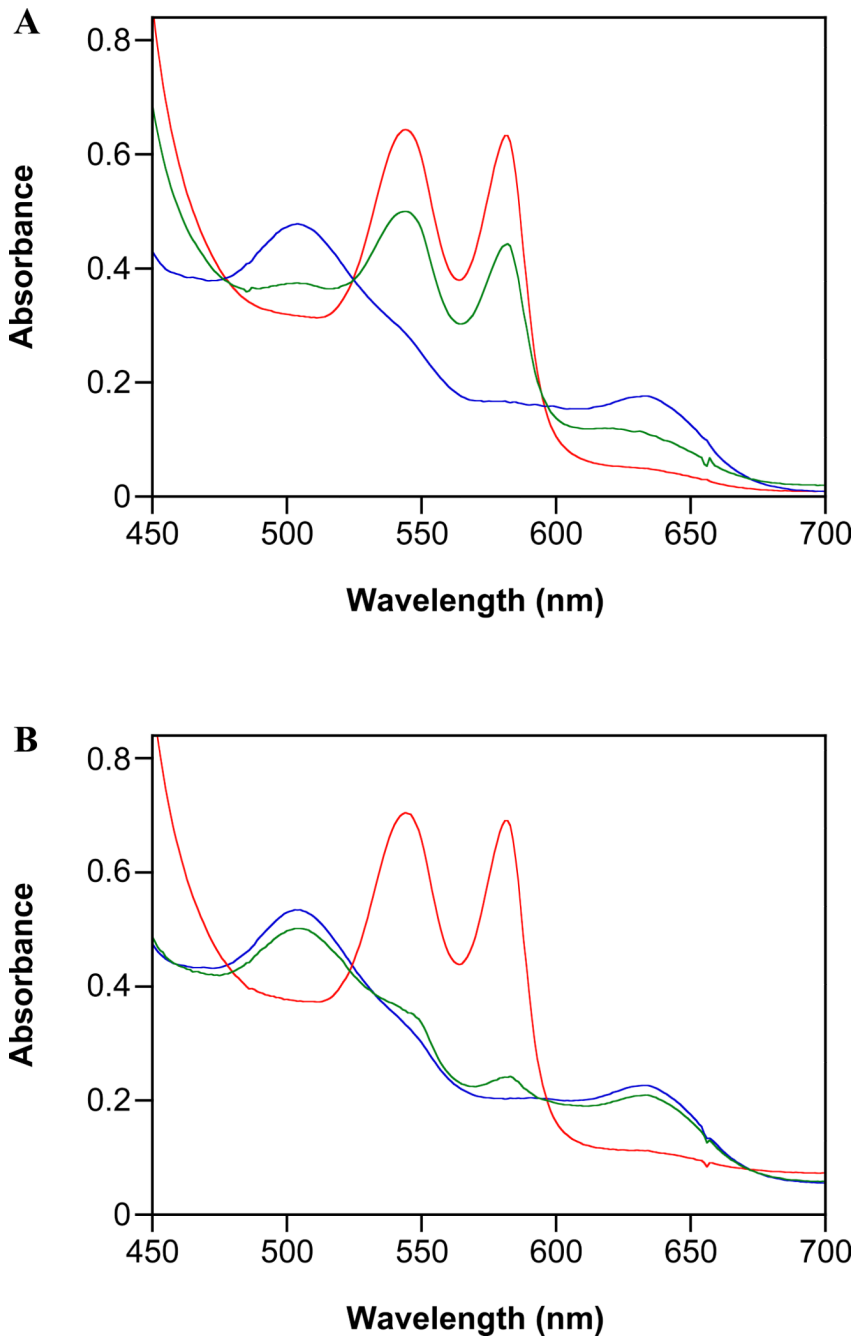

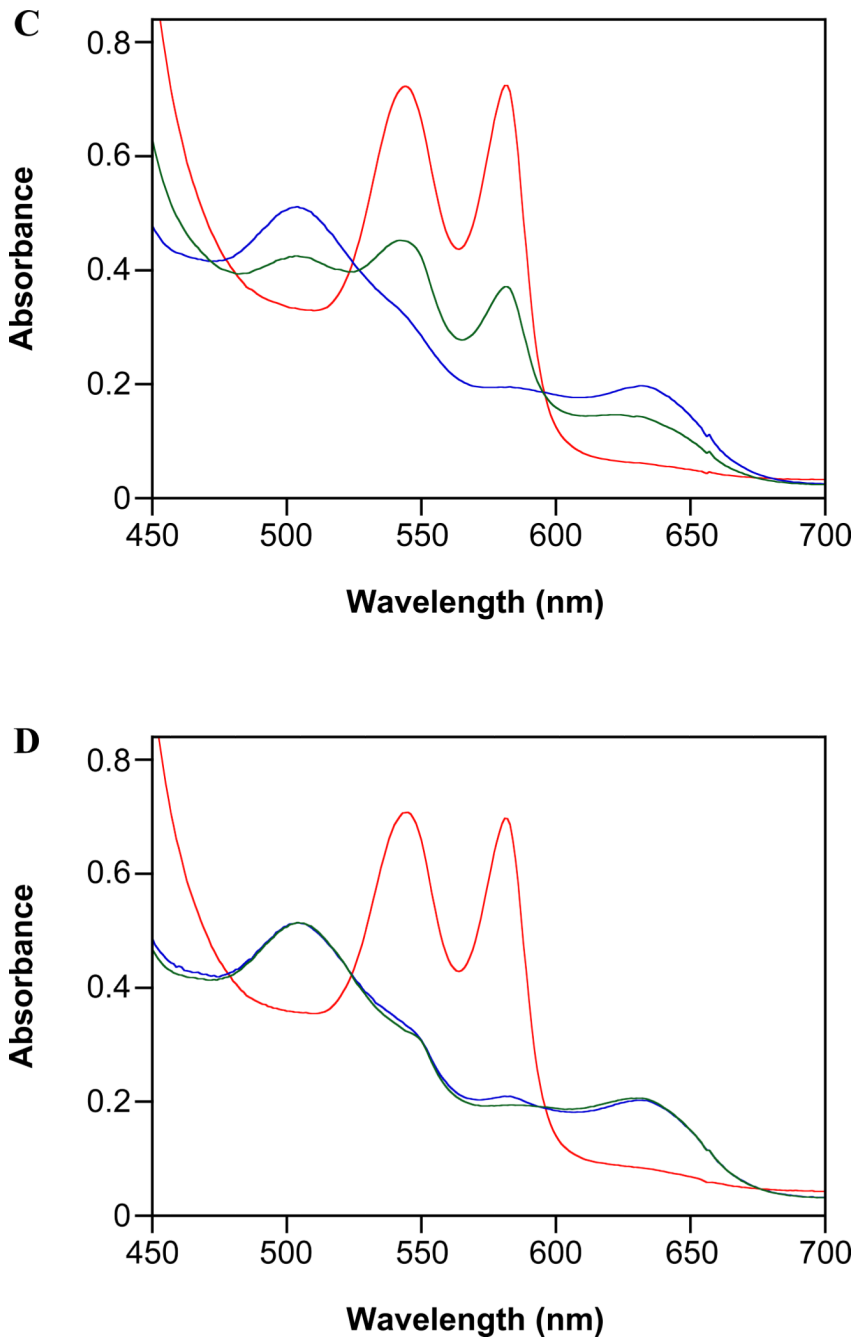

Figure 4.

Representative spectral changes ($n \geq 3$) indicating trapping of NO and HNO by MbO_2 (50 μM) during decomposition at 37°C of IPA/NO-aspirin or DEA/NO-aspirin in assay buffer ± GSH (1 mM): (**A**) 250 μM IPA/NO-aspirin, (**B**) 250 μM DEA/NO-aspirin, (**C**) 100 μM IPA/NO-aspirin + 2% guinea pig serum and (**D**) 50 μM DEA/NO-aspirin (given production of 2 eqs of NO) + 2% guinea pig serum. Initial scans are in red (MbO_2), final scans without GSH are in blue (155 min for **A**; 350 min for **B**; 1170 s for **C**; and 600 s for **D**) and final scans with GSH are in green (145 min for **A**; 210 min for **B**; 1170 s for **C**; and 690 s for **D**).

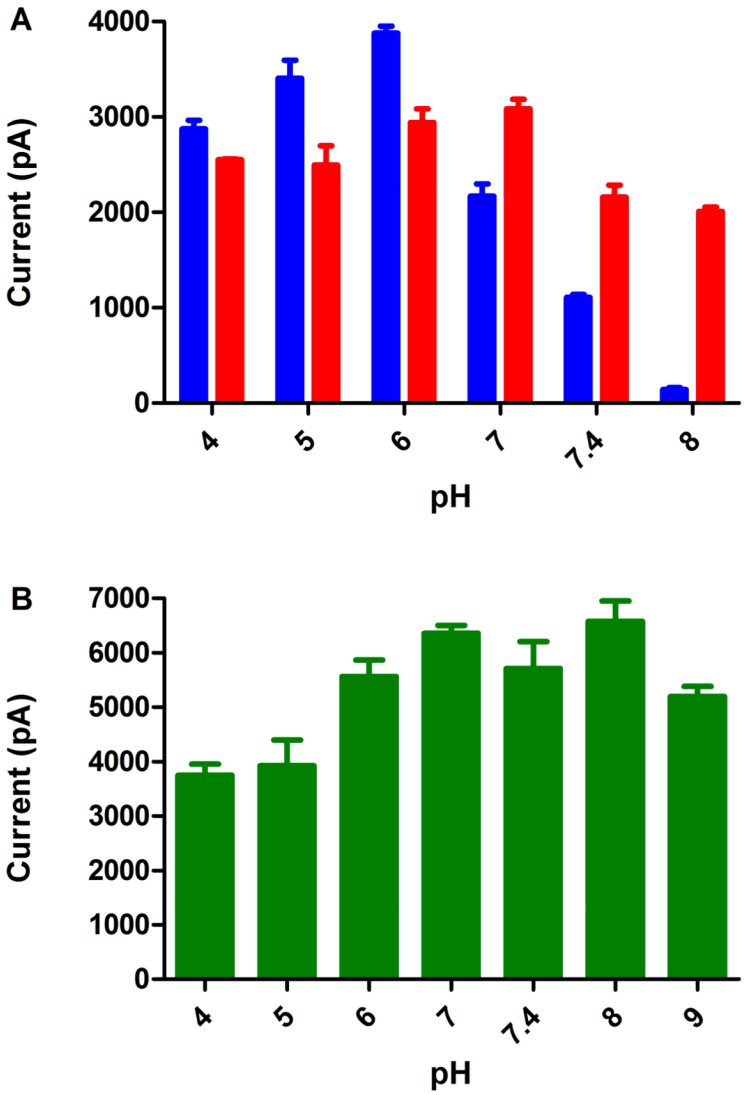

Figure 5.

Maximum current intensity from an NO-specific electrode as a measure of NO and HNO release from 100 μM of (**A**) IPA/NO-aspirin or (**B**) DEA/NO-aspirin in assay buffer containing 2% guinea pig serum (in **A**, blue bars in assay buffer alone and green bars with addition of 1 mM ferricyanide. The data are expressed as mean ± SD ($n \geq 3$).

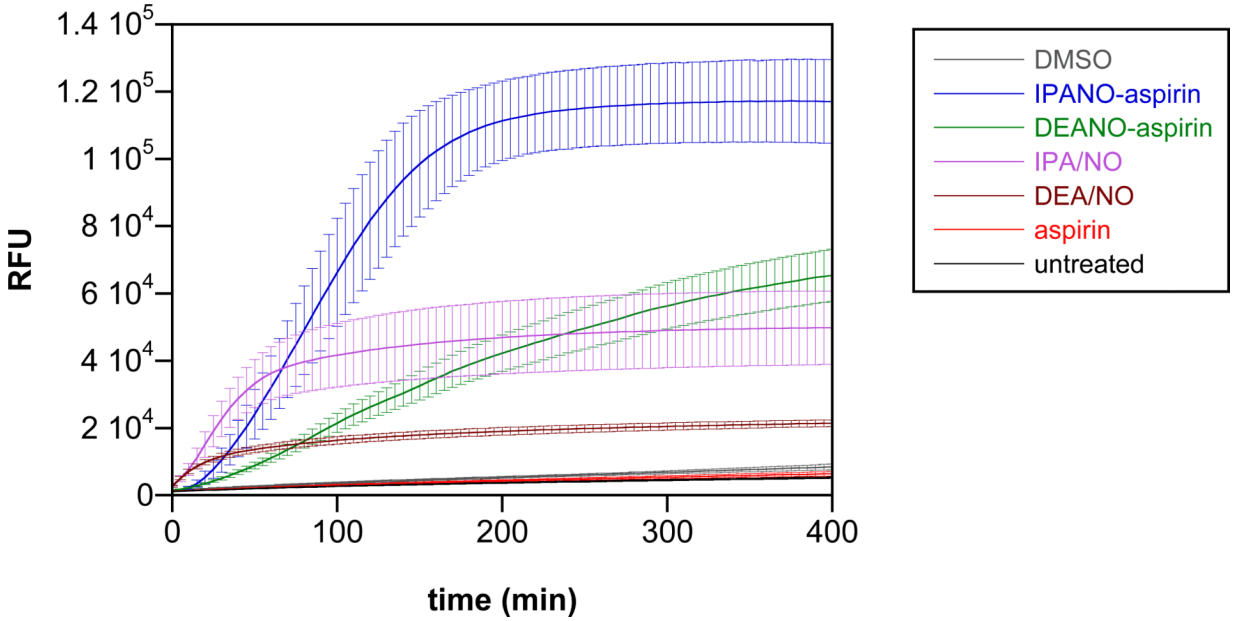

Figure 6.

NO and HNO release measured in A549 cells. The cells were exposed 100 μL of 10 μM DAF-2DA in PBS pH 7.4 for 75 min at 37°C and washed three times with PBS pH 7.4 to remove excess dye. Upon addition of 10 μM of DEA/NO-aspirin, IPA/NO-aspirin or aspirin in DMSO (<0.1%), 10 μM IPA/NO or DEA/NO in 10 mM NaOH or DMSO (n = 2, six replicates per plate), the increase in fluorescence intensity at 535 nm was measured as a function of time at 37°C following excitation at 485 nm. The data are expressed as mean ± SD.

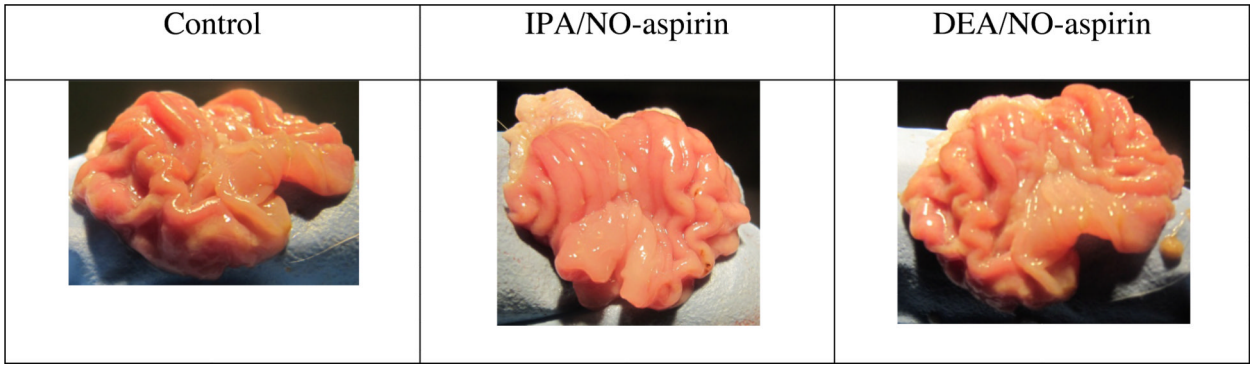

Figure 7.
Examination of the stomach ulcerogenicity of IPA/NO-aspirin and DEA/NO-aspirin (1.38 mmol/kg). Ulcerogenicity was not significantly increased compared to control.

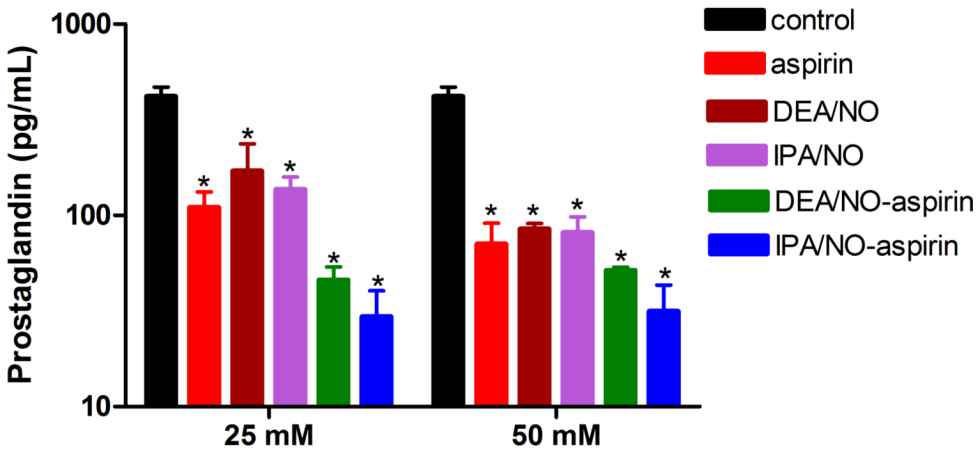

Figure 8.

Effect of IPA/NO-aspirin, DEA/NO-aspirin, IPA/NO, DEA/NO and aspirin (25 and 50 μM) on PGE_2 levels after 24 h exposure to A549 cells (experiment in triplicate; *, $p < 0.001$ vs. control) at 37°C.

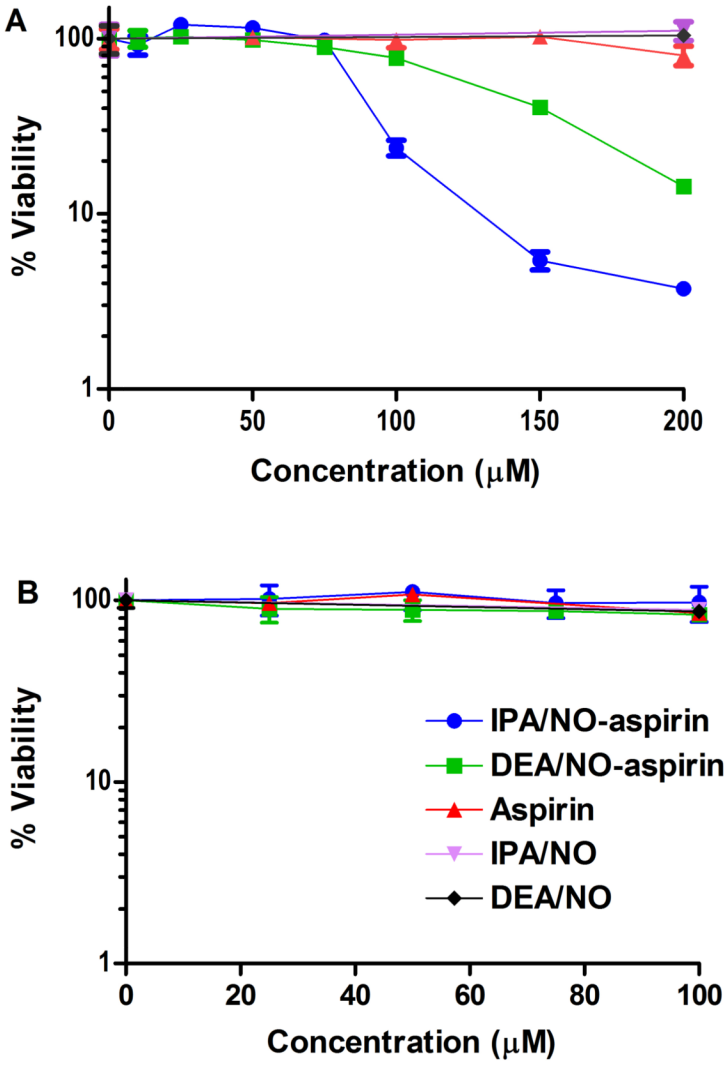

Figure 9.

The effect of NONO-aspirin prodrugs and appropriate controls (10-200 and 25-100 μM, respectively) on cell viability of (**A**) A549 and (**B**) HUVEC cells. Cells were treated for 48 h at 37°C and then analyzed by the spectrophotometric MTT assay (n = 3 for A549s and n = 1 for HUVECs in at least triplicate per plate).

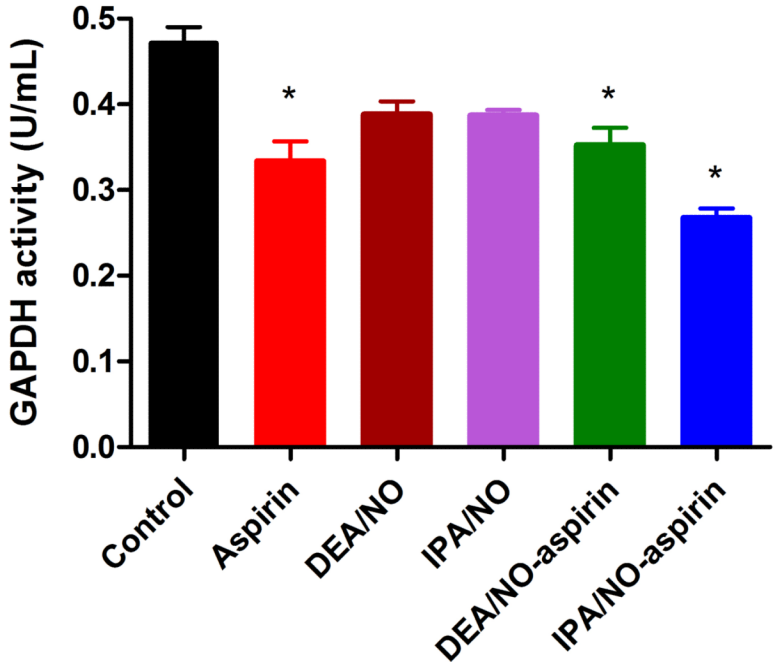

Figure 10.

Effect of IPA/NO-aspirin, DEA/NO-aspirin, IPA/NO, DEA/NO and aspirin (100 μM) on GAPDH activity in A549 cells at 1 h (experiment in triplicate) at 37°C. The data are expressed as mean ± SD (experiment in triplicate), and one-way ANOVA was applied to determine the significance of the difference between control and treatment groups (*, $p < 0.01$).

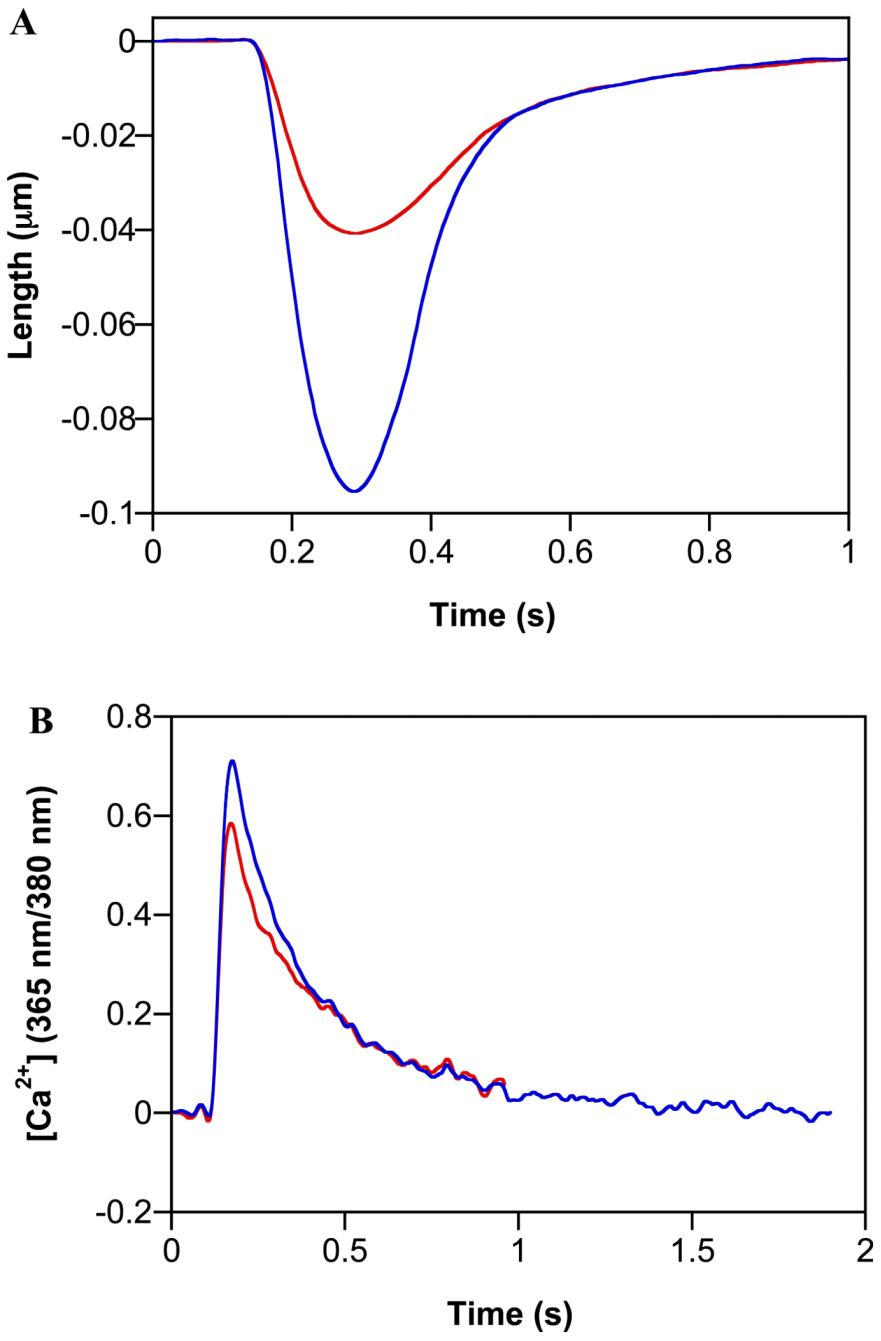

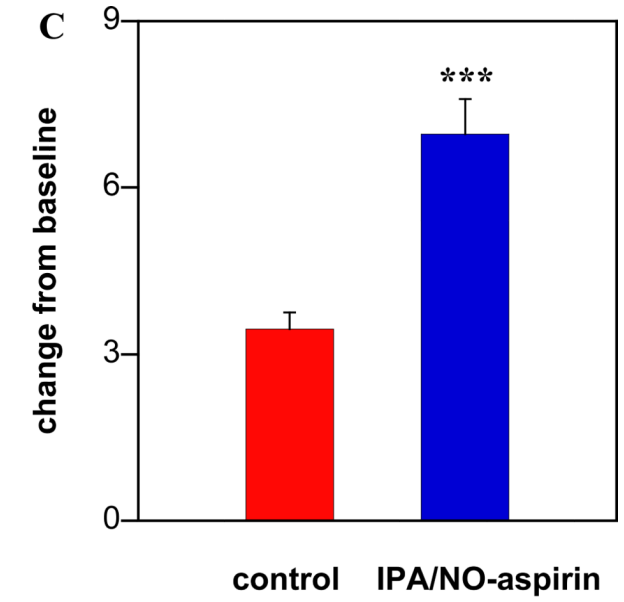

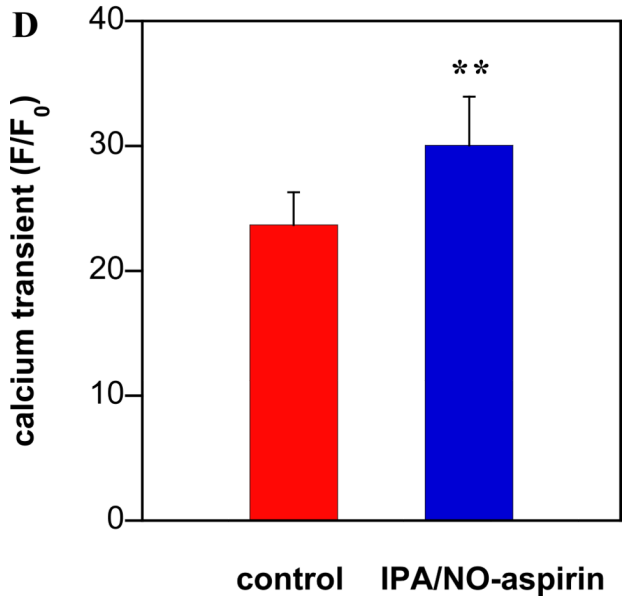

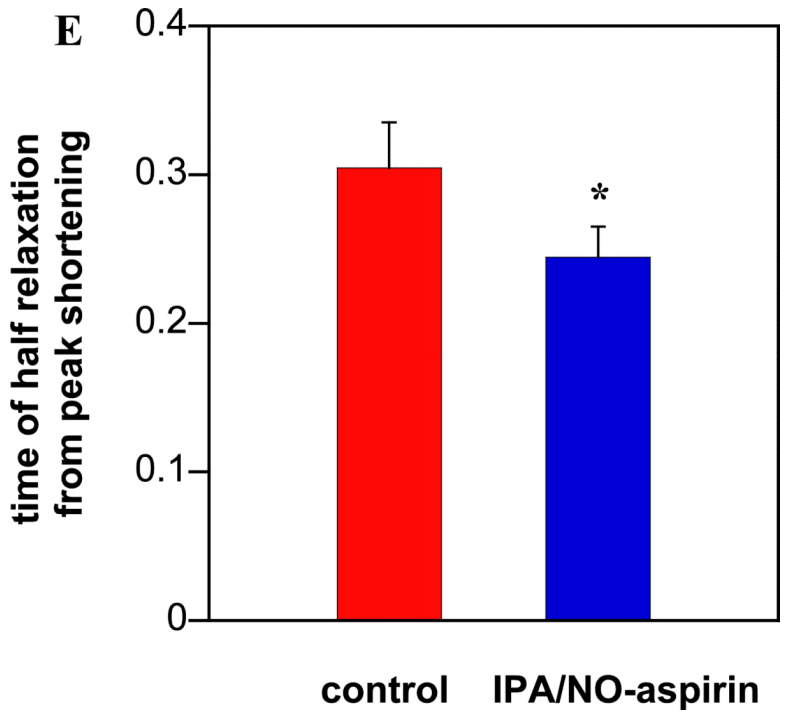

Figure 11.

The effect of IPA/NO-aspirin (500 μm) on contractility and relaxation in isolated ventricular myocytes (IPA/NO-aspirin in blue compared to control in red): (**A**) representative trace of sarcomere length (μm), (**B**) representative trace of calcium transient (ratio 365 nm/380 nm), (**C**) absolute changes in sarcomere shortening (n = 12 cells), (**D**) calcium transients and (**E**) myocyte relaxation (time of half relaxation from peak shortening (t_{50}). The data are expressed as mean ± SEM (*, $p < 0.005$; **, $p < 0.001$; ***, $p < 0.0001$).